




Gene expression and characterization of clonally derived murine embryonic brown and brite adipocytes

Cristina Velez-delValle , Claudia Patricia Hernandez-Mosqueira, Lidia Itzel Castro-Rodriguez, Alfredo Vazquez-Sandoval , Meytha Marsch-Moreno and Walid Kuri-Harcuch 

Department of Cell Biology, Center for Research and Advanced Studies (Cinvestav), Mexico City, Mexico

Keywords

adipocytes; adipogenesis; brite/beige; brown; differentiation; gene expression

Correspondence

W. Kuri-Harcuch, Department of Cell Biology, Center for Research and Advanced Studies (Cinvestav), Apdo. Postal 14-740, Mexico City 07000, Mexico
Tel: +52 55 57473353
E-mail: walidkuri@cinvestav.mx

(Received 12 January 2024, revised 29 May 2024, accepted 25 June 2024)

doi:10.1002/2211-5463.13861

White adipocytes store energy, while brown and brite adipocytes release heat via nonshivering thermogenesis. In this study, we characterized two murine embryonic clonal preadipocyte lines, EB5 and EB7, each displaying unique gene marker expression profiles. EB5 cells differentiate into brown adipocytes, whereas EB7 cells into brite (also known as beige) adipocytes. To draw a comprehensive comparison, we contrasted the gene expression patterns, adipogenic capacity, as well as carbohydrate and lipid metabolism of these cells to that of F442A, a well-known white preadipocyte and adipocyte model. We found that commitment to differentiation in both EB5 and EB7 cells can be induced by 3-Isobutyl-1-methylxanthine/dexamethasone (Mix/Dex) and staurosporine/dexamethasone (St/Dex) treatments. Additionally, the administration of rosiglitazone significantly enhances the brown and brite adipocyte phenotypes. Our data also reveal the involvement of a series of genes in the transcriptional cascade guiding adipogenesis, pinpointing GSK3 β as a critical regulator for both EB5 and EB7 adipogenesis. In a developmental context, we observe that, akin to brown fat progenitors, brite fat progenitors make their appearance in murine development by 11–12 days of gestation or potentially earlier. This result contributes to our understanding of adipocyte lineage specification during embryonic development. In conclusion, EB5 and EB7 cell lines are valuable for research into adipocyte biology, providing insights into the differentiation and development of brown and beige adipocytes. Furthermore, they could be useful for the characterization of drugs targeting energy balance for the treatment of obesity and metabolic diseases.

Abbreviations

ACC2, acetyl-CoA carboxylase 2; Atgl, adipose triglyceride lipase; BAT, brown adipose tissue; BRT, “brown in white” adipose tissue; Cd81, cluster of differentiation 81; CEB/P α , CCAAT/enhancer binding protein alpha; CEB/P β , CCAAT/enhancer binding protein beta; ChREBP, carbohydrate response element binding protein; CIDE-A, cell death activator; Cpt1b, palmitoyl-CoA transferase-1b; Dex, dexamethasone; DMEM, Dulbecco’s Modified Eagle’s Medium; FABP4, fatty acid binding protein 4; Fasn, fatty acid synthase; GLUT4, glucose transporter 4; GPD1, glycerophosphate dehydrogenase; GSK3 β , glycogen synthase kinase-3 beta; HSL, hormone sensitive lipase; Lhx8, LIM homeobox protein 8; LPL, lipoprotein lipase; Mix, 3-isobutyl-1-methylxanthine; MUFA, mono unsaturated fatty acids; Myf-5, myogenic factor 5; NAd, nonadipogenic medium; PDGFR α , platelet-derived growth factor receptor alpha; Pparg2, peroxisome proliferator activated receptor gamma 2; Ppargc1 α , peroxisome proliferative activated receptor gamma coactivator 1 alpha; PRDM16, PR domain zinc finger protein 16; RMD, 1 μ M rosiglitazone, 0.5 mM mix, and 1 μ M Dex; Rplp0, ribosomal phosphoprotein large P0; Sca1, spinocerebellar ataxia type 1; Scd1, stearoyl-CoA desaturase-1; SDR, St/Dex/Ros; SREBP1c, sterol regulatory element-binding protein 1 isoform c; St, staurosporine; Tcf21, transcription factor 21; Tmem26, transmembrane protein 26; UCP1, uncoupling protein 1; WAT, white adipose tissue; Zic1, zinc finger protein of the cerebellum 1; β_3 -Ars, β_3 -adrenergic receptors.

Adipose tissues are highly dynamic organs that play a central role in metabolic and energy homeostasis. White, brown, and brite (beige) adipocytes have important metabolic properties that contribute to whole-body metabolic regulation, reviewed in Scheele and Wolfrum [1].

In rodents, brown adipocytes are pronounced in the interscapular fat depots and are derived from a cell lineage characterized by *Myf-5*⁺ (Myogenic factor 5) skeletal muscle-like cells [2]. Beige or brite adipocytes have brown adipocyte activity and are found in predominantly white adipose tissue (WAT) and near the blood vessels. Their cell progenitors reside within the vasculature among the mural cells are not derived from the *Myf-5*⁺ lineage [3], thus making them genetically distinct from brown fat. Brown adipose tissue (BAT) and “brown in white” adipose tissue (BRT) are thought to be suitable targets for obesity therapy because of their ability to regulate energy expenditure. Excess fats can be broken down by lipid oxidation and provide fuel for thermogenesis in mitochondria of brown and brite adipocytes. The fatty acids released into the circulation from WAT and those from the brown and brite adipocytes lipid stores are fuel sources for thermogenesis. BAT burns excess lipids through obligatory and nonshivering thermogenesis, while BRT burns excess lipids through nonshivering thermogenesis in response to chronic cold exposure and by β_3 -adrenergic stimuli; some estimates indicate that in the human body brite are more abundant than brown adipocytes [4–8].

Brown and brite adipocytes carry out thermogenesis through Uncoupling protein 1 (UCP1), the uncoupling respiratory protein at the mitochondrial inner membrane. Basal UCP1 expression is higher in brown fat cells than in brite, and lowest in white adipocytes [9]. Brown- and brite-mediated energy expenditure can improve glucose and lipid homeostasis through increased fatty acid beta-oxidation and thermogenesis [10–13, reviewed by 14]. This raises the possibility to treat obesity through increasing mass and/or stimulating the activity of BAT and/or BRT (i.e., browning or briteing) [8,15]. The observation that BAT mass or/and activity is reduced during aging and in subjects with obesity and diabetes [16], it also suggests that increasing BAT and BRT mass or activity might lead to promising therapies for those diseases.

Several proteins regulate adipogenesis of brown and brite fat cell progenitors. PR Domain Zinc Finger Protein 16 (PRDM16), a transcriptional zinc-finger histone methyltransferase expressed in brown and beige adipocytes, as well as in smooth muscle cells and a few other tissues, controls the thermogenic program in brown and brite adipocytes [11]. In mouse embryos of 9–12 days

gestation, PRDM16 controls the muscle-brown fat differentiation decision in the *Myf-5*⁺ progenitors, and its expression leads to brown adipogenesis [2,17,18]. In the mouse embryo brown fat arises at 9–12 days of gestation, whereas subcutaneous WAT arises at 14–18 days [19]. Adult WAT has brite fat progenitors likely derived from *Myf-5*-precursors expressing platelet-derived growth factor receptor alpha (PDGFR α ⁺) [8,19–21], and a subset of progenitors marked by PDGFR α , Spinocerebellar ataxia type 1 (*Scal*), and Cluster of Differentiation 81 (*Cd81*) [22]. While it is well established that brown and white adipocyte progenitors originate during embryonic life, the developmental timing of brite progenitors remains unclear, whether they emerge during embryonic stages or postnatally.

Brown and brite adipocyte models have been investigated in humans, animals, virally immortalized cell lines, and in primary cell cultures from BAT and from the stromal-vascular fraction of adipose tissue [23–25]. Brite adipose cell culture models are less common than those of brown adipose, which limit research into the molecular regulation of BRT differentiation and function. Despite that PRDM16 is expressed in mouse embryos, limited studies of brown or brite adipogenesis have been reported in embryonic cellular models [2,17,18]. While the C3H10T1/2 cell line was established from 14- to 17-day-old mouse embryos [26] and has been used to study brown adipogenesis [27–29] and expression of select beige markers [30–34], detailed genetic and cold-response analysis related to the beige phenotype is lacking.

Research with cell cultures can aid in a better understanding of the mechanisms that regulate brown and brite cell differentiation and metabolism, which, in turn, may lead to new treatments for metabolic diseases. Thus, to better understand adipogenesis and early development of brown and brite adipocytes, we established cell culture models of these cells using previously derived cells from 11- to 12-day murine embryos [35]. Following the derivation protocol used for the white 3T3-F442A (F442A) preadipocytes [36,37], we derived two adipogenic clonal cell lines EB5 and EB7 from mouse strain NMRI embryos.

de Jong *et al.* [38] described experiments using adipose tissues from brown (interscapular), brite (inguinal), and white (epididymal) regions of NMRI mice, along with primary cell cultures derived from these tissues, to assess various genetic markers. Most of these markers (*Car4*, *Cited1*, *Ebf3*, *Eva1*, *Fbxo31*, *Fgf21*, *Lhx8*, *Hoxc8*, and *Hoxc9*) were not strongly indicative of tissue type. However, markers such as *Zic1* (specific to brown adipose tissue), *Cd137*, *Epsti1*, *Tbx1*, *Tmem26* (associated with brite adipose tissue), and

Tcf21 (indicative of white adipose tissue) were informative for distinguishing between these tissues. Notably, *Lhx8* expression was significantly higher in interscapular BAT compared to inguinal BRT and was undetectable in epididymal WAT. *Lhx8* is found in brown and only seen in brite when this tissue is activated with β -adrenergic agonists [38,39]. The study also acknowledges discrepancies in marker reliability reported in the literature, suggesting that variations could be due to factors such as mouse strain differences (C57BL/6 versus NMRI), cell culture conditions, among others. Consequently, we used a subset of these genetic markers previously reported for the NMRI strain [38] to evaluate the EB5 and EB7 clones, which originated from NMRI mice.

We examined the expression profiles of the genetic markers: Zinc finger protein of the cerebellum 1 (*Zic1*) and LIM homeobox protein 8 (*Lhx8*) for brown, Transmembrane protein 26 (*Tmem26*) for brown and brite, and Transcription factor 21 (*Tcf21*) for white. The limitations of genetic marker analysis in providing a definitive identification of adipocyte lineage, as noted by de Jong *et al.*, led us to complement our study with an assessment of the clones' response to cold exposure [40]. Integrating the genetic and the response to cold data enabled us to identify the lineage of the EB5 and EB7 clones, each with the ability to differentiate into adipocytes under appropriate culture conditions.

The expression of carbohydrate and lipid metabolic genes in brown and brite cultured adipocytes is not well known. Carbohydrate, lipogenic, and lipolytic pathways are important in providing fatty acids into the mitochondria for thermogenesis in BAT and BRT. Glucose might be available through the GLUT4 transporter, while the fatty acids are available through the following metabolic pathways: (a) Fatty acid uptake from the bloodstream via triglyceride degradation into fatty acids and glycerol by lipoprotein lipase and lipolysis from the intracytoplasmic triglycerides. (b) Lipogenesis, or the *de novo* fatty acids synthesis and triglycerides. (c) Intracytoplasmic fatty acid transport. (d) Mono-unsaturated fatty acid synthesis. To get a better understanding of these metabolic pathways in brown and brite adipocytes, we determined the expression levels of select genes that encode crucial enzymes within these pathways in EB5, EB7, and F442A adipocytes: For fatty acid uptake, the genes encoding lipoprotein lipase (LPL, gene *Lpl*) and the intracellular lipolytic proteins, adipose triglyceride lipase (*Atgl*, gene *Atgl*), and hormone-sensitive lipase (*Lipe*, gene *Lipe*). For lipogenic enzymes, fatty acid synthase (*Fasn*, gene *Fasn*), glycerophosphate dehydrogenase (*Gpd1*, gene *Gpd1*), and *Mlxipl*, the gene encoding for carbohydrate response element binding protein

(ChREBP), a helix–loop–helix leucine zipper transcription factor. For transporters, the genes encoding the glucose transporter (GLUT4, gene *Slc2a4*), the intracytoplasmic fatty acid transporters (FABP4, gene *Fabp4*), and CD36 (gene *Cd36*). For beta-oxidation, *Cpt1b* that encodes the enzyme palmitoyl-CoA transferase-1b, a fatty acid transporter into the mitochondria that is in the outer mitochondrial membrane and essential for thermogenesis. An important regulator of CPT1b activity is malonyl-CoA Acetyl-CoA Carboxylase 2 (*ACC2*, gene *Acacb*) catalyzes the formation of malonyl-CoA, an inhibitor of CPT1b activity. For mono-unsaturated fatty acid synthesis, the rate-limiting enzyme, stearoyl-CoA desaturase-1 (*Scd1*, gene *Scd1*) that catalyzes the biosynthesis of Mono Unsaturated Fatty Acids (MUFA), palmitoleyl-CoA, and oleyl-CoA from palmitoyl-CoA and stearoyl-CoA, respectively. MUFA are key components of triglycerides and membrane phospholipids, as well as precursors for fat oxidation and thermogenesis. For adipokines, adiponectin (*Adipoq*) and leptin (*Lep*).

The β_3 -adrenergic response indicates brown adipocytes physiological capabilities. Upon rodents' exposure to cold, the sympathetic nervous system releases norepinephrine, a β_3 -adrenergic agent, and activates nonshivering thermogenesis in the brown adipocytes through β_3 -Adrenergic receptors (β_3 -ARs) [41].

Basal respiration is low in brown adipocytes, but norepinephrine stimulation of β_3 -ARs in brown adipocytes increased adenylyl cyclase activity, lipolysis, and oxygen consumption (thermogenesis) through increased UCP1 transcript and activity [41–47]. Silencing β_3 -ARs reduced all of them and the expression of genes involved in fatty acid metabolism, mitochondrial mass, and thermogenesis, as well [48]. Lipolysis is crucial for UCP1 activation. *Atgl* and HSL lipases inhibition completely blocked the adrenergic thermogenic response [49]. UCP1 knock-down adipocytes did not initiate thermogenesis in response to β_3 -adrenergic receptor agonists, but still showed norepinephrine-induced lipolysis, indicating that UCP1 is the sole mediator of adrenergic-induced thermogenesis [49]. Activation of β_3 -adrenergic receptors lead to lipolysis, increased *Ucp1* expression, uncoupled respiration, and fatty acid metabolism.

The response of brown adipocytes to norepinephrine provides insight into their metabolic and functional states beyond the scope of metabolic gene expression. We assessed lipolysis and UCP1 content in EB5 and EB7 adipocytes following norepinephrine stimulation to evaluate their metabolic and functional competence.

Taken together, our findings highlight the potential to map differentiation, disease, and drug pathways in a rapid and robust manner by doing comparative

studies with the three types of white, brown, and brite preadipocytes and adipocytes in culture.

Methods

Materials

We obtained Dulbecco's Modified Eagle's Medium (DMEM) and TRIzol[®] reagent from Thermo Fisher Scientific (Waltham, MA, USA). Both calf and adult bovine serum were sourced from HyClone (Logan, UT, USA), a subsidiary of Thermo Fisher Scientific. Adult cat serum was collected from domestic adult cats in strict compliance with the guidelines set forth in the Guide for the Care and Use of Laboratory Animals of the National Institutes of Health. All animal handling procedures were conducted in accordance with protocols approved by the Internal Committee for the Care and Use of Laboratory Animals (CICUAL) at of the Center for Advanced Research (CINVESTAV-IPN). Epidermal growth factor was procured from Upstate Inc. (Charlottesville, VA, USA). Additional reagents such as insulin, D-biotin, human transferrin, triiodothyronine, dexamethasone, 3-Isobutyl-1-methylxanthine, rosiglitazone, staurosporine, SB415286, and Oil Red O were obtained from Sigma-Aldrich. (Saint Louis, MO, USA). All other chemicals used in the experiments were of analytical grade.

Cell culture and isolation of the EB5 and EB7 preadipocytes

We previously established a parental cell line from 11 to 12 days NMRI mouse embryos through a regimen of subculture transfers, adhering to protocols previously used for 3T3 cells derived from Swiss mouse embryos [50]. Due to the age of the mouse embryos, we hypothesized that this line could contain brown adipocyte progenitor cells. To investigate this, two successive cloning steps were carried out. Initially, the parental cells were cultured in DMEM supplemented with 10% calf serum. These growing cultures were then trypsinized and seeded at 100 cells per dish into two 100-mm tissue culture dishes. This led to the derivation of adipogenic clonal cells EB5 and EB7, following methodologies established for white F442A preadipocytes [36,37]. Once colonies achieved a small yet confluent center, they were subjected to 48 h treatment with an RMD medium. This medium consisted of 1 μM Rosiglitazone, 0.5 mM 3-Isobutyl-1-methylxanthine, and 1 μM dexamethasone (RMD), and was further supplemented with 5 $\mu\text{g}\cdot\text{mL}^{-1}$ insulin, 1 μM D-biotin, and 2 nM triiodothyronine.

After 48 h in RMD medium, we switched the cultures to a nonadipogenic medium. We proceeded to isolate 20 colonies exhibiting various degrees of adipose differentiation using cloning cylinders, following established protocols [36,37]. These isolated colonies were then subcultured into 35-mm tissue culture dishes. Prior to reaching confluence,

cells were transferred to a 100-mm tissue culture dish containing growth medium. Out of these, only two clones—designated as EB5 and EB7—were selected based on their elevated levels of adipose differentiation. This was determined by Oil Red O staining for intracellular lipid accumulation, as depicted in Fig. 1A. This figure also includes some of the other clones that demonstrated lower levels of adipose differentiation for comparative purposes.

In alignment with our previous work on F442A cells, which demonstrated that less than 48 h of induction with a differentiation cocktail is sufficient for cellular commitment to differentiation [51,52], we adopted a similar approach for the three clones under study. The F442A cells were cultured in nonadipogenic medium (NAd), consisting of DMEM supplemented with 2.5% adult cat serum, 2.5% adult bovine serum, 5 $\mu\text{g}\cdot\text{mL}^{-1}$ insulin, and 1 μM D-biotin; we previously found that cat serum is nonadipogenic for the F442A cells [53]. Two days after reaching confluence, the medium was switched to an adipogenic medium for 48 h. This adipogenic medium was DMEM supplemented with 4% adult cat serum, 1% adult bovine serum, 5 $\mu\text{g}\cdot\text{mL}^{-1}$ insulin, 5 $\mu\text{g}\cdot\text{mL}^{-1}$ transferrin, 1 μM D-biotin, 2 nM triiodothyronine, and RMD.

For the EB5 and EB7 clones, they were initially grown in NAd medium, which included DMEM supplemented with 5% bovine calf serum that we found is nonadipogenic for these clones. Upon reaching confluence, we replaced the medium with adipogenic medium (comprising 5% bovine calf serum, 5 $\mu\text{g}\cdot\text{mL}^{-1}$ insulin, 5 $\mu\text{g}\cdot\text{mL}^{-1}$ transferrin, 1 μM D-biotin, and 2 nM triiodothyronine) containing RMD for a 48-h period. Subsequently, the cultures were reverted back to NAd medium to undergo terminal differentiation, unless otherwise specified. All cultures were maintained at 37 °C in a 10% CO₂ atmosphere. At the end of the experiment, cells were fixed overnight in 4% formalin and stained with Oil Red O to assess lipid accumulation [54].

To investigate the involvement of GSK3 β in the differentiation process of the F442A, EB5, and EB7 clones, we conducted parallel experiments. The cells were cultured as previously described and were subjected to treatment with or without the GSK3 β selective inhibitor, 100 μM SB415286, for 24 h during the adipogenic induction phase. The vehicle control cultures contained 1% DMSO.

For cold response assays, F442A, EB5, and EB7 cells were cultured until mature adipocytes formed, which occurred 8 days postdifferentiation induction. Following this, the culture medium was replaced, and after a 2-h incubation, the cells were exposed to a 30 °C and 10% CO₂ environment for 4 h. The cultures were then washed twice with PBS at 30 °C before being frozen.

Mouse tissues

Male newborn C57BL/6 mice were sourced from the unit of production of experimental animals (UPEAL) at

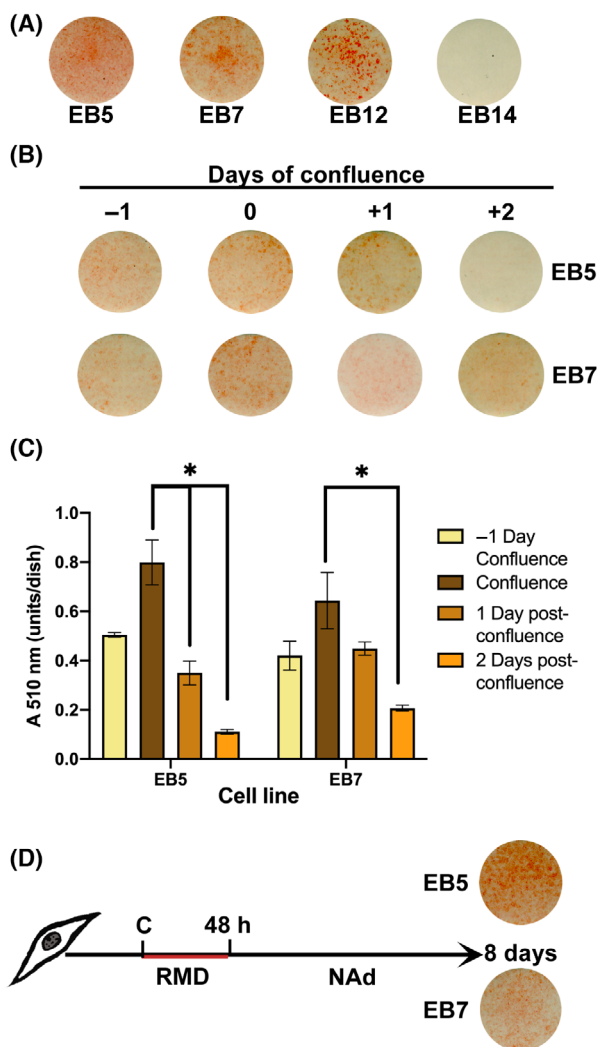


Fig. 1. Murine embryonic clonal cell lines. Clones were cultured and induced to differentiation with RMD for 48 h and stained with Oil-Red-O at terminal differentiation to show lipid accumulation. (A) Four clones shown with different levels of lipid accumulation for comparative purposes, among them the EB5 and EB7 selected clones for their highest level of adipose differentiation. (B) The EB5 and EB7 cell cultures were stimulated at different days of confluence with RMD for 48 h to determine the optimal time of confluence for adipose induction. (C) Quantitation of Oil Red O staining of cultures shown in B. (D) The provided image is a schematic of the standardized cell culture protocol using RMD to induce adipogenesis, which was applied across all assays. NAd, nonadipogenic medium; RMD, 1 μM Rosiglitazone, 0.5 mM 3-Isobutyl-1-methylxanthine, and 1 μM dexamethasone. The results are given as the mean SEM of two triplicate experiments ($n=6$). ANOVA was used to establish statistical differences, indicated with an asterisk with a P value lower than 0.05.

CINVESTAV-IPN. Following cervical dislocation for euthanasia, in compliance with UPEAL-CINVESTAV-IPN institutional guidelines, tissues were promptly dissected and

snap-frozen in liquid nitrogen. Entire tissue depots were collected for analysis.

Analysis of gene expression

We extracted total RNA with TRIzol[®] reagent, as described by the manufacturer. We transcribed 1 μg of total RNA into cDNA using oligodT primer, and SuperScript II[™] reverse transcriptase reaction mix (Invitrogen, Carlsbad, CA, USA) according to the manufacturer's instructions. Relative quantitative real-time PCR (RT-PCR) was carried out with FastStart Universal SYBR Green I Master (Rox) kit (Roche Applied Science, Mannheim, Germany). We monitored the reaction amplification on a CFX96[™] Real-Time PCR Detection System BIORAD (Bio-Rad, Hercules, CA, USA). The specific primers for each gene are listed in Table 1. We determined the expression values using the $2^{-\Delta C_T}$ equation, and we normalized each gene expression to that of the ribosomal phosphoprotein large P0 (*Rplp0*) gene that was amplified from the same sample. In each experiment we compared each gene from the three clones, and we show gene expression as relative changes. The amplification products were separated in 1.5% (w/v) agarose gel. We verified the identity of all amplification products by sequencing, using an ABI PRISM[™] 310 DNA Sequencer (PerkinElmer, Boston, MA, USA) and the Big Dye Terminator kit v3.1 (PerkinElmer). We compared the sequencing data with the reference GeneBank data [55] using the BLASTN 2.2.30 suite [56]. We used the names and acronyms of proteins and genes accordingly to the NCBI GenBank and GenPept databases (Table S1).

The acronyms denoting the murine proteins and genes are according to the Mouse Genome Informatic (MGI).

Lipolysis measurement

EB5 and EB7 preadipocytes were seeded at a density of 1×10^3 cells cm^{-2} , and differentiation was initiated using RMD, as described above. After terminal differentiation, we switched to phenol red-free DMEM supplemented with 5% calf serum, insulin, biotin, transferrin, and triiodothyronine. As lipolytic stimuli, we used 5 μM L-Norepinephrine hydrochloride (Sigma-Aldrich) for 7 h. We collected the media and used the Free Glycerol Determination Kit (Sigma-Aldrich) to determine the free glycerol, following the manufacturer's instructions. We measured absorbance at 540 nm with a Biotech[®] Synergy[™] HT reader (Agilent, Santa Clara, CA, USA). The data are expressed as nmoles of glycerol per mg of protein [57].

Immunoblotting

We lysed the cultures in a buffer containing 50 mM Tris-HCl pH 7.5, 150 mM NaCl, 0.5% NP-40, and 0.1% SDS, plus Complete[®] protease inhibitor (Roche Applied Science).

Table 1. Primers used for this study

Gene	Accession number	Sequence	T_a (°C)	Product size (bp)	Source
<i>Acacb</i>	NM_133904	CACCATTTTCAGCAAGCCCACTAT GGCCGCACAGCTCATCTATCAG	61.4	157	This work
<i>Adipoq</i>	NM_009605	CAATGGCACACCAGGCCGTGAT CCAGCCCACACTGAACGCTGA	69.5	212	[95]
<i>Atgl</i>	NM_025802	CAAGGGGTGCGCTATGTGGATGG GAGGCGGTAGAGATTGCGAAGGTT	58	189	[57]
<i>Cd36</i>	NM_001159558	TGGCCTTACTGGGATTGG CCAGTGTATATGTAGGCTCATCCA	58	111	[57]
<i>Cebpa</i>	NM_007678	GAGTCGGCCGACTTCTACG GTCTCGTGCTCGCAGATGC	62	178	[64]
<i>Cebpb</i>	NM_009883	CCGCGCACACCAGACTTCCCCT CGCTCGCGCCGCATCTTGTA	61	451	[64]
<i>Cidea</i>	NM_007702	TCATCAGGCCCTGACATTC CCAGGCCAGTTGTGATGACT	57.4	186	This work
<i>Cpt1b</i>	NM_009948	TTCCAAACGTCACTGCCTAAG TTCCCACAGTCACTCACATAG	60	213	This work
<i>Fabp4</i>	NM_024406	AAGAGAAAACGAGATGGTGACAA CTTGTGGAAGTCACGCCTTT	62	65	[64]
<i>Fasn</i>	NM_007988	TTGGGGGCGTGAGATGTGTTG CCTCGGGTGTGGTGGGTTTG	60.9	106	This work
<i>Gpd1</i>	NM_010271	CTGAGATCATCAACACTCAGC TGTCAGCGCCTGTTGCAGC	60	111	[57]
<i>Lep</i>	NM_008493	GAGCGGGATCAGGTTTTGTGGT TGTCCTTTTCCCCTCTCTTCA	64.5	161	[95]
<i>Lhx8</i>	NM_010713	GGCCCGCCATAAGAAACACG TGGGGTAAACAAGGGCTGGAGTC	64.4	203	This work
<i>Lipe</i>	NM_010719	TGCCAGCGCCTGTGACCA CGCCAGGCCAAGCAGGAGTCAAAC	62	260	[57]
<i>Lpl</i>	NM_008509	ATGCAGAAGCCCCAGTCGC CCAGCTGGTCCACGCTCTCCGA	62	149	This work
<i>Mlxipl</i>	NM_021455	AACGGAGGAAGAGCCAGTGT CGGAGCCGCTTTTGTAGTAGA	63.3	172	This work
<i>Myf5</i>	NM_008656	AGGAGCTGCTGAGGGAACA CTGGACACGGAGCTTTTATCTG	63	205	This work
<i>Ppargc1a</i>	NM_008904	TCCTCCCAACTCCTCCTCATAA GATTGCTCGGGCCCTTTCTTG	63.4	171	This work
<i>Pparg2</i>	NM_011146	TCGCTGATGCACTGCCTATG GAGAGGTCCACAGAGCTGATT	60.0	60	[96]
<i>Prdm16</i>	NM_027504	CAGCACGGTGAAGCCATTC GGGAGGAGGTAGTGTGAACATCT	60.0	149	This work
<i>Rplp0</i>	NM_007475	AGGCCCTGCACTCTCGCTTTCTGG TGTTCCCTTTGGCGGGATTAGTCG	60.0	347	[52]
<i>Scd1</i>	NM_009127	CGAGGGCTCCACAACCTACC AACTCAGAAGCCCCAAAGCTCA	55.1	130	This work
<i>Slc2a4</i>	NM_009204	ACCGGCTGGGCTGATGTGTCTGA TATGGTGGCGTAGGCTGGCTGTCC	63	240	[57]
<i>Srebf1a</i>	NM_011480	TAGTCCGAAGCCGGGTGGGCGCCGCAT GATGTCGTTCAAAACCGCTGTGTGTCCAGTTC	60	106	[97]
<i>Srebf1c</i>	NM_011480	ATCGGCGCGGAAGCTGTGGGGTAGCGTC CTGTCTTGGTTGTTGATGAGCTGGAGCAT	63	116	[97]
<i>Tcf21</i>	NM_011545	ACCTGACGTGGCCCTTTATGGT GTGTTCTTGGGGGTGGGATAG	60.3	230	This work
<i>Tmem26</i>	NM_177794	GTCATCCACAGAGCCACCAAT GCCGTCCCACAAAACATCAG	65.0	216	This work

Table 1. (Continued)

Gene	Accession number	Sequence	T_a (°C)	Product size (bp)	Source
<i>Ucp1</i>	NM_009463	GGATTGGCCTCTACGACTCA TGACAGTAAATGGCAGGGGA	60.4	380	This work
<i>Zic1</i>	NM_009573	CTGGCTGCGGCAAGGTTTTC GAGCTGGGGTGCGTGTAGGACT	63.2	208	This work

The gene names are displayed in italics.

We separated 70 µg of protein from the extracts using 12.5% SDS/PAGE and immunoblotted them with rabbit polyclonal anti-UCP1 (AB23841; Abcam Limited, Cambridge, UK), as reported by Kiefer *et al.* [58] overnight at 4 °C and POX polyclonal goat anti-Rabbit (111035003; Jackson ImmunoResearch Inc, WestGrove, PA, USA) for 1 h at room temperature. The proteins were evidenced by chemiluminescent HRP substrate Immobilon™ Western (Millipore, Billerica, MA, USA) and detected with the Odyssey® Fc Imaging System (LI-COR Biosciences, Lincoln, NE, USA) IMAGE STUDIO v. 5.2.

Data presentation and statistical analysis

Data are presented as mean ± standard error, derived from six or more cultures across two to three separate experimental runs. Statistical comparisons were made using a two-tailed Student's *t*-test for two groups and analysis of variance (ANOVA) for three or more groups, utilizing GRAPHPAD PRISM v. 9.0.1 (GraphPad Software, Boston, MA, USA) for macOS. A *P* value of ≤0.05 was considered statistically significant. Qualitative data corresponds to one representative experiment done in triplicate.

Results

The EB5 and EB7 cells express gene markers for brown and brite fat cell lineages, respectively

Most of the studies promote adipose differentiation by adding the adipogenic cocktail at 2 days after confluence. The two clones EB5 and EB7, isolated as described in [Methods](#), undergo adipose differentiation by adding RMD in the culture medium. The optimal time to add RMD for 48 h was the confluence day, since induction 1 day before, or 1 or 2 days after confluence, resulted in a lower differentiation than the day of confluence. Quantitation of Oil Red staining of intracellular lipids [54] correlated with the stained culture dishes (Fig. 1A–C). After incubation with RMD, the cultures were kept with NAd for an additional 6 days until terminal differentiation (Fig. 1D).

To identify the adipose phenotype of the EB5 and EB7 clones we determined, by RT-PCR, the expression of the genes widely accepted as typical for each

adipose tissue, as previously described [38,39]. We determined by RT-PCR the expression of the lineage genetic markers *Tcf21* (white), *Zic1* (brown), *Myf5* (brown fat progenitors) [2], *Lhx8* (brown), *Tmem26* (brown and brite), *Prdm16* (brown and brite), and the expression of brown and brite fat functional genes, Cell death activator *Cidea*, and *Ucp1* [38,39]. We extracted the RNA from iBAT; eWAT for brite and white fat genes. Yet, eWAT has precursors of brite adipocytes and undergo browning by cold exposure or when adipocytes in culture are treated with rosiglitazone [38,49,59]. Figure 2 shows that each gene was expressed according to the tissue reported data. *Myf5* seemed to be expressed in eWAT and muscle; however, sequencing of each amplicon showed that the band in both muscle (M) and brown fat (BF) was indeed a *bona fide Myf5* band, but not that in eWAT (Fig. 2, gel electrophoresis panel of amplicon). For *Zic1* we used brain tissue as a control to validate gene expression, consistent with published data indicating high levels of *Zic1* in brain.

The expression of some of the brown and brite genes in eWAT might be due to some browning of eWAT during tissue manipulation. Then we determined by RT-PCR the expression of genes in each clone regarded as typical genes expressed in muscle and epididymal and brown adipose tissues (Fig. 2) [38,39].

Peroxisome proliferator activated receptor gamma 2 (*Pparg2*) expression was used as the adipogenic gene marker. We chose *Rplp0*, the ribosomal phosphoprotein large P0 protein, as the reference gene since it did not show any statistically significant difference in the three clones under the used culture conditions (Fig. 3Aa).

The three cell lines cultured in NAd medium and induced with RMD highly expressed the adipocytes marker *Pparg2*, whereas those preadipocytes cultured with NAd did not express *Pparg2* (Fig. 3Ab). *Prdm16*, a brown and brite marker gene, was equally expressed in EB5 and EB7 preadipocytes and adipocytes, but not expressed in F442A (Fig. 3Ac). *Tcf21* expression was low in EB5 and EB7 preadipocytes and adipocytes, but high in F442A preadipocytes, but not in adipocytes (Fig. 3Ad). The EB5 preadipocytes expressed the widely accepted brown marker *Lhx8* that was

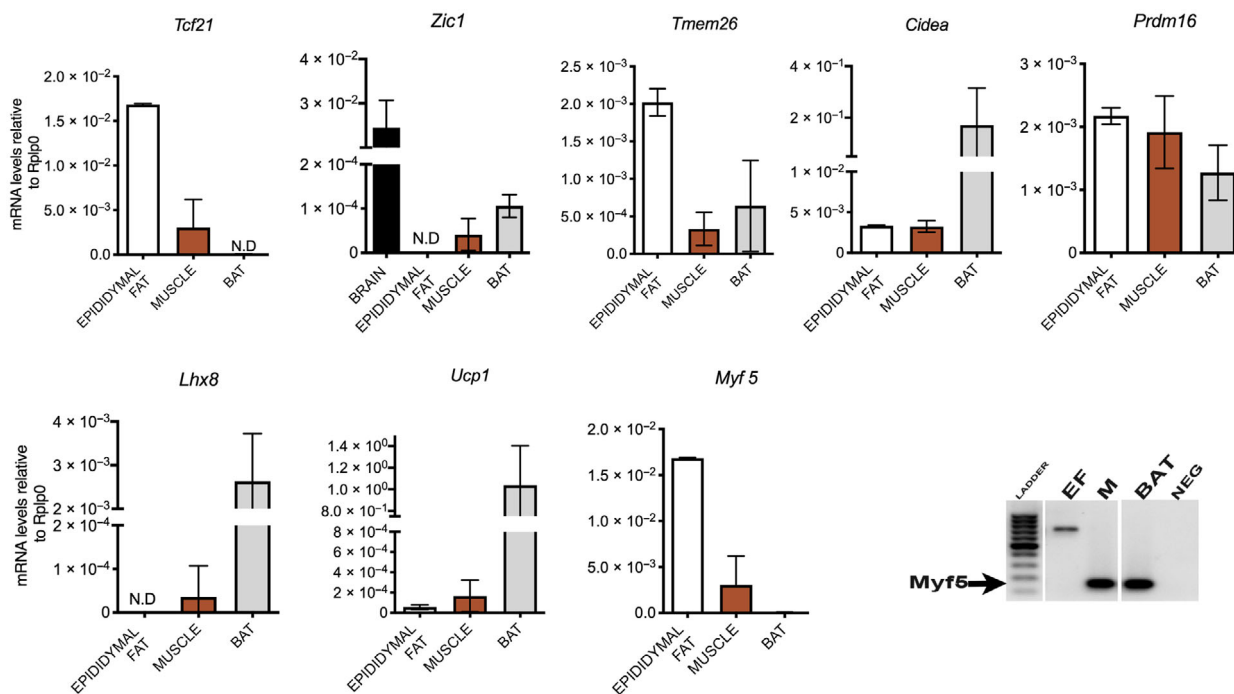
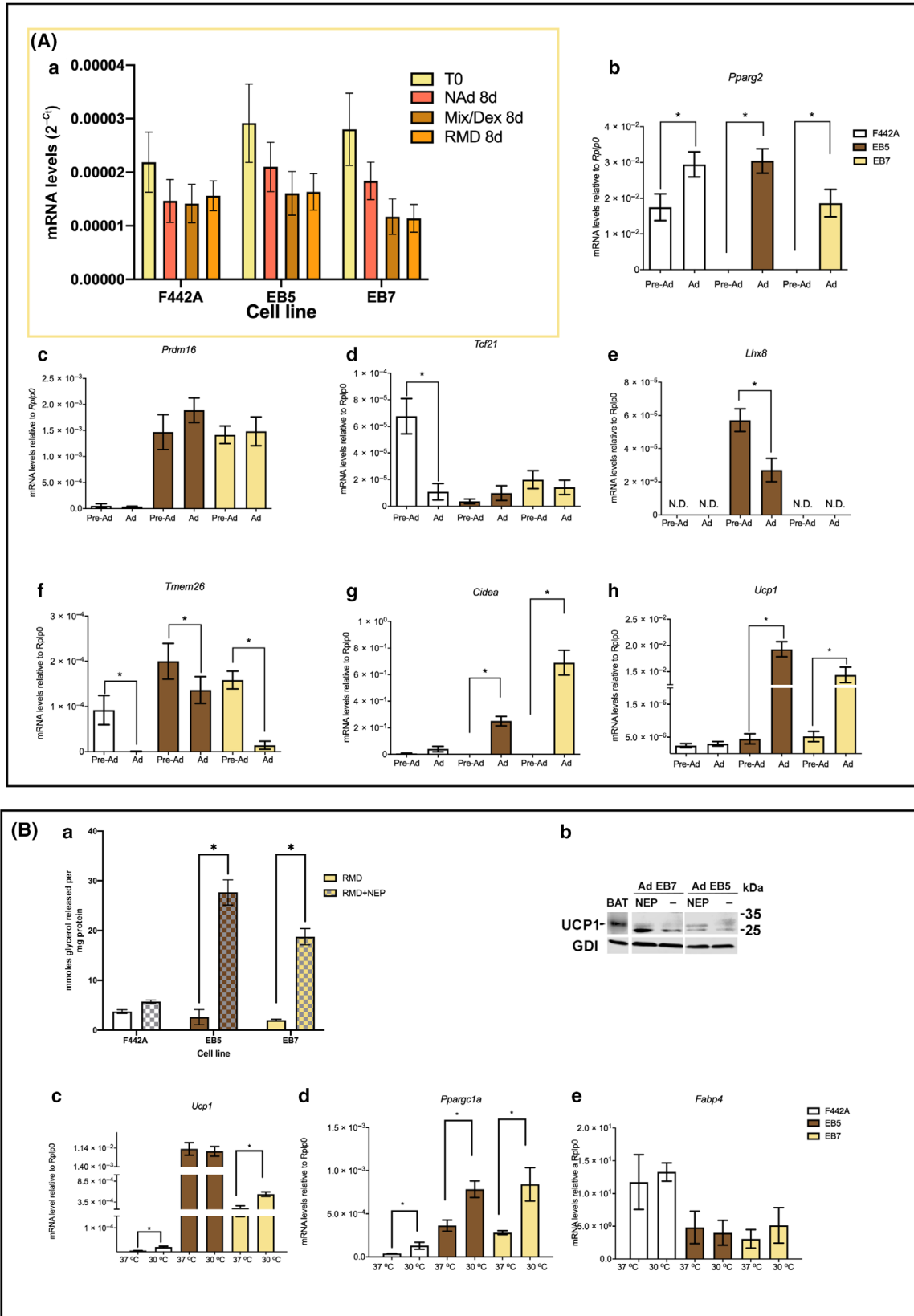


Fig. 2. Expression of the genes widely accepted as typical markers for brown, brite, and white adipose tissues. RNA was extracted from mouse tissue samples, brain, muscle (M), epididymal (EF), and brown fat (BF), and we carried out RT-PCR to determine gene expression. The *Myf 5* amplicon band is shown in the gel electrophoresis panel. ThermoFisher ultra-low-range DNA ladder is shown in lane 1. The results are given as the mean SEM of two experiments.

downregulated in the adipocytes, but its expression was undetectable in the EB7 and F442A preadipocytes and adipocytes (Fig. 3Ae). *Tmem26* was highly expressed in EB5 and EB7 preadipocytes, EB5 adipocytes expressed *Tmem26* greater than EB7 adipocytes, and F442A preadipocytes, but not adipocytes expressed *Tmem26* (Fig. 3Af). EB5 and EB7 adipocytes, but not preadipocytes, and neither F442A preadipocytes nor adipocytes, expressed *Cidea* and *Ucp1*, the thermogenic genes (Fig. 3Ag,h). In all clones, *Myf5* and *Zic1* expression was undetectable. Together, these results strongly suggested that EB5 are brown preadipocytes, since they express *Lhx8*, a brown selective gene. The EB7 are brite preadipocytes, since they

did not express *Lhx8*, but they did express *Tmem26*, a brown and brite selective gene. Both EB5 and EB7 adipocytes expressed *Ucp1* and *Cidea*. The F442A preadipocytes are of the white adipose lineage and they expressed *Tcf1*, but did not express *Cidea* and *Ucp1*. Since *Myf5* and *Zic1* expression was undetectable, we did not explore the mechanisms of the early progenitor development, since by the cloning methodology, most likely, the isolated clones have already passed the early progenitor stages. For example, EB5 cells represent initial-stage brown preadipocytes, having successfully transitioned beyond the progenitor phase, characterized by the expression of *Myf5* and *Zic1*, but may be positioned within a subsequent phase of development,

Fig. 3. (A) Adipose marker gene expression from EB5, EB7, and F442A cells. EB5 and EB7 cultures were treated at confluence, and F442A at 2 days postconfluence, for 48 h with NAd, Mix/Dex, or RMD, and gene expression was measured using RT-PCR. (a) Expression of *Rplp0*; (b) Expression of *Pparg2*; (c–h) Expression of the lineage specific markers *Prdm16*, *Tcf21*, *Lhx8*, *Tmem26*, *Cidea*, and *Ucp1*. (B) Physiological response to β_3 -adrenergics and gene expression after cold exposure. (a) Lipolysis assay. Adipocyte cultures were incubated for 7 h with $5 \mu\text{M}$ L-norepinephrine hydrochloride. Lipolysis was measured as glycerol release. (b) UCP1 WB. Seventy micrograms of proteins obtained from cultures stimulated with $5 \mu\text{M}$ L-norepinephrine hydrochloride was used to immunoblot UCP1. (c–e) Cold response. Adipocyte cultures induced with RMD were incubated at 30°C for 4 h, and the expression of *Ucp1*, *Pparg1a*, and *Fabp4* genes was measured using RT-PCR. The results are given as the mean SEM of two triplicate experiments ($n=6$). Asterisks indicate statistical differences with a P value ≤ 0.05 , evaluated by ANOVA, except for *Lhx8* where T student was used.



distinguished by the expression of the brown preadipocyte marker *Lhx8*. As for the cellular progenitors of the ‘brite’ lineage, it has been observed that these cells express *Prdm16* [60], a trait similarly exhibited by the EB7 clone (akin to EB5). This pattern could indicate that EB7 cells constitute early-stage brite preadipocytes.

Physiological response to norepinephrine of the EB5 and EB7 adipocytes

We treated the EB5 and EB7 adipocytes with 5 μ M norepinephrine and determined lipolysis by a glycerol release assay and UCP1 content by immunoblotting, as a response to the β_3 -adrenergic stimulation. Norepinephrine stimulated lipolysis by at least 18-fold in the EB5 and EB7 adipocytes relative to untreated cells; but it did not significantly stimulate the F442A white adipocytes (Fig. 3Ba). Immunoblotting of UCP1 by a specific antibody revealed that norepinephrine concomitantly increased UCP1 protein content in EB5 and EB7 adipocytes (Fig. 3Bb). Our results align with previous observations that showed norepinephrine increased oxygen consumption, expression of *Ucp1* mRNA, and lipolysis, as described above (see Introduction). Our results point out that EB5 and EB7 adipocytes are physiologically competent.

The response to cold supports that EB5 are brown and EB7 are brite adipocytes

Interscapular brown fat in mice exposed to cold (4 °C) temperatures for 2 h increased the expression of *Ppargc1a* but not of *Ucp1* [61]. The 3T3-L1 and F442A white adipocytes and a cultured brite adipocyte clones exposed to 27–33 °C for 4 h increased *Ucp1* and Peroxisome proliferative activated receptor gamma coactivator 1 alpha (*Ppargc1a*) expression, responding to cold stimuli, while a brown fat clonal line did not; cold also did not increase cytosolic Fatty acid binding protein 4 (*Fabp4*) gene expression [8,40]. Based on our genetic marker data, we have inferred that the EB5 clone is derived from a brown fat lineage, whereas the EB7 clone is associated with the brite fat lineage. To confirm the identification suggested by the genetic markers, we conducted experiments to assess the expression of functional genes, *Ucp1*, *Ppargc1a*, and *Fabp4*, in response to cold exposure, as previously described by Ye *et al.* [40]. We incubated the adipocyte cultures at 30 °C for 4 h. Cold incubation increased *Ucp1* expression in F442A and EB7 adipocytes, and increased *Ppargc1a* expression in the three types of adipocytes. While cold did not increase *Ucp1*

expression in EB5 adipocytes, it is worth noting that *Ucp1* expression was already elevated in these cells prior to cold exposure. Under unstimulated conditions, brown adipocytes have relatively higher levels of *Ucp1* than beige adipocytes. Cold had no effect on *Fabp4* expression in any of the three adipocytes studied (Fig. 3Bc–e). These results, integrated with those on the lineage gene expression described above, support the conclusion that the EB5 clone is indeed of the brown lineage and EB7 of the brite lineage.

Mix/Dex and St/Dex induce commitment to differentiation, and rosiglitazone stimulates the brown and brite adipose phenotype expression

The study of induction or commitment to differentiation into adipocytes is paramount to understanding the early mechanisms of adipogenesis. Small drug-like molecules added to cells cultured in NAd medium can facilitate the study of the early expression of genes and molecular pathways leading to commitment. For example, they offer the advantage of altering signaling pathways that are otherwise regulated by endogenous serum adipogenic proteins. Differentiation of the white 3T3-L1 and F442A cells depends on adipogenic serum supplemented to the culture medium [53]. Mix/Dex are a common cocktail that enhances adipogenesis in cells cultured in medium supplemented with adipogenic serum [62]. Mix inhibits phosphodiesterases, and blocks the inhibitory regulatory protein G_i and stimulates adenylyl cyclase activity [63]. Furthermore, Staurosporine (St) rapidly induced commitment to differentiation of F442A cells during only 4 h incubation in nonadipogenic or serum-free medium; Dex did not induce it but enhanced adipose conversion [52,64]. St, a serine/threonine kinase inhibitor, activates GSK3 β by promoting its dephosphorylation in Ser^{21/9} [65]. Mix/Dex combined with rosiglitazone (Ros), an agonist of PPAR γ , have been used to differentiate brown and brite preadipocytes. Ros stimulates “browning” in white subcutaneous adipose tissue and in primary cultures of adipocytes from murine BAT [66,67]. However, no studies have been done with Mix/Dex or St/Dex to induce differentiation of brown or brite cells cultured in NAd or serum-free medium.

We thought it of interest to induce commitment of brown and brite adipocyte differentiation with these small molecules. RMD or St/Dex/Ros (SDR) induced rapidly the differentiation of the EB5 and EB7 cells cultured in NAd medium; EB5 were induced by 2 h and B7 by 24 h (Fig. 4Aa–c). The EB5 and EB7 cells treated with Mix/Dex, St/Dex, or Ros alone did not undergo morphological changes or accumulate

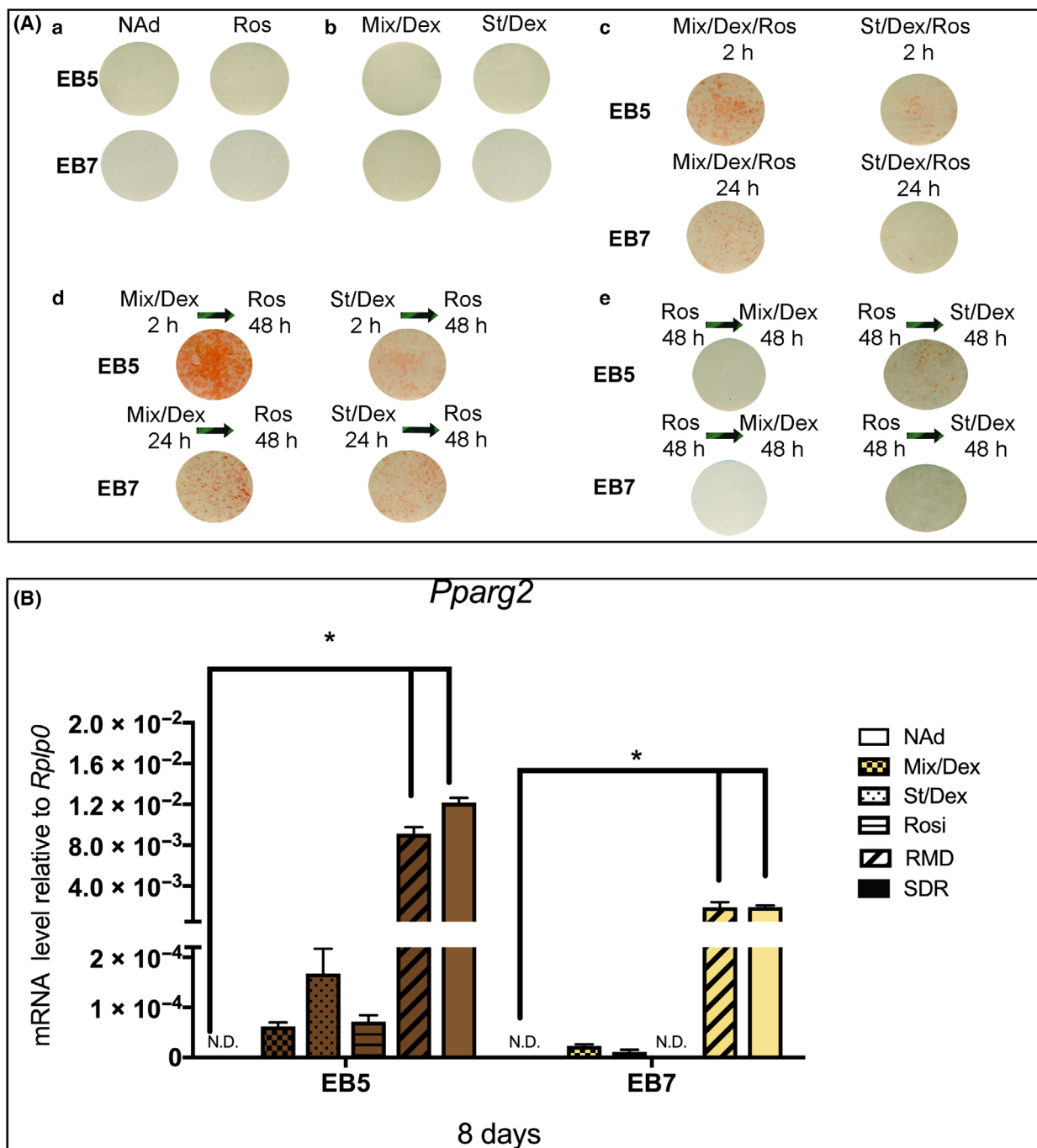


Fig. 4. (A) Effect of Mix/Dex, St/Dex, and Ros on commitment to differentiation. (a) Representative photographs of adipose conversion from confluent cultures of EB5 and EB7 cells treated for 48 h with NAd or Ros. Cultures were followed up to 192 h and stained with Oil Red O; (b) Similar cultures as in a, but treated with Mix/Dex or St/Dex; (c) Confluent cultures induced by 2 h for EB5 and 24 h for EB7 with RMD or SDR; (d) Confluent cultures induced by 2 h for EB5 and 24 h for EB7 with Mix/Dex or St/Dex and then stimulated for 48 h with Ros; (e) Cultures treated by 48 h with Ros and stimulated with Mix/Dex or St/Dex for 24 h. (B) Cultures, treated for 48 h with each stimulus, were harvested at 192 h. Gene expression was assessed by RT-PCR. The data are presented as the mean ± SEM of two triplicate experiments (*n* = 6). Asterisks indicate statistical differences between the indicated data groups with a *P* value ≤ 0.05, evaluated by ANOVA.

intracellular lipids, and they remained with a fibroblastic morphology (not shown), as did cells cultured in NAd (Fig. 4Aa,b). However, EB5 and EB7 cells first treated with Mix/Dex or St/Dex, as described above, and then followed with only Ros for up to 48 h underwent adipose differentiation (Fig. 4Ad), while cells treated with Ros for 48 h and then with Mix/Dex or St/Dex did not differentiate (Fig. 4Ae).

We examined the expression changes of *Pparg2* in cells treated with RMD or SDR. *Pparg2* highly increased its expression in differentiated adipocytes of both EB5 and EB7 cells (Fig. 4B). Parallel cultures treated with Mix/Dex or St/Dex without Ros or only with Ros did not express *Pparg2*, similar to cells cultured in NAd medium (Fig. 4B). Altogether, these results showed that Mix/Dex and St/Dex induced commitment or primed the EB5 and EB7 cells to undergo adipogenesis, remaining with fibroblastic morphology, but they needed Ros to undergo phenotypic expression and terminal differentiation into adipocytes. Ros by itself did not induce differentiation. Since this adipose model can separate Mix/Dex or St/Dex from Ros action, it provides valuable information needed to study early genes expressed during preadipocyte commitment and later genes expressed in the brown or brite adipocyte.

The adipogenic transcriptional cascade in brown, brite, and white adipocytes

Differentiation of white preadipocytes involves a complex activity of transcription factors; including CCAAT/enhancer binding protein (C/EBP) beta (CEB/β), PPARγ2, CCAAT/enhancer binding protein alpha (CEB/α), Sterol regulatory element-binding protein 1 isoform c (SREBP1c) [60,68,69], and some members of the Kruppel family of transcription factors [70–72]. We previously reported a temporal relationship in the expression of the genes encoding the transcription factors during F442A cells adipogenesis [64]. *Srebf1a* was expressed shortly after *Cebpb* and silencing of *Srebf1a* blocked adipose differentiation as well as the expression of *Pparg2*, *Cebpa*, and *Srebf1c*, indicating its crucial role during white adipogenesis [64]. The brown and brite adipogenic gene expression is not fully studied. Therefore, we examined the gene expression in EB5 and EB7 cells during differentiation at various culture times.

The time-course expression of *Cebpb*, *Pparg2*, *Cebpa*, and *Srebf1c* in EB5 (Fig. 5A) and EB7 (Fig. 5B) cells treated with RMD was similar to that seen in F442A cells cultured in adipogenic conditions [64]. *Cebpb* was expressed early and transiently, reaching its maximum at 4 and 8 h for EB5 and EB7, respectively (Fig. 5Aa, Bg). *Pparg2*, *Cebpa*, and *Srebf1c* expression began later

than that of *Cebpb*, reaching its maximum at the mature adipocyte state in both cell lines (Fig. 5Ab–d, Bh–j). *Srebf1a* expression did not increase in EB5, but it significantly did in EB7 at 24 h before decreasing to the NAd low levels in the adipocytes (Fig. 5Ae,Bk); *Srebf1a* increased its expression early in F442A cells and remained high up to terminal differentiation [64].

CIDE-A is a lipid droplet protein that is shuttled to the nucleus, where it acts transcriptionally to drive UCP1 expression through promoting PPARγ binding to a *Ucp1* enhancer element in human adipocyte brite-nig [73]. CIDE-A gene expression increased after the genes of the adipogenic transcriptional cascade and well during adipose terminal differentiation in EB5 and EB7 cells (Fig. 5Af,C). *Ucp1* was also expressed at the adipose stage (Fig. 3Ah). The results showed the expression of the genes encoding some of the key transcription factors during white adipocyte differentiation occurs in the EB5 and EB7 cells as well. The most significant difference was the expression of *Srebf1a*, which did not seem to have a crucial role in brown, but it likely does in brite fat adipogenesis, as in white fat cells. EB5 and EB7 cells treated with Mix/Dex without Ros did not express any of these genes (Fig. 5Ae,Bk), accordingly to our data described above.

GSK3β regulates EB5 and EB7 adipogenesis

GSK3β is a well-described regulator of adipogenesis and the transcriptional cascade in white adipogenesis [64,74] and has been proposed to be a negative regulator of the adrenergic-mediated thermogenic program in brown adipocytes [75]. The role of GSK3β in brite cells has not been reported. We interrogated whether activation of GSK3β is also a crucial early event in the brown and brite transcriptional pathways. We cultured the EB5 and EB7 cells as described above, and at confluence, we induced the cultures with RMD or SDR. We treated parallel cultures with the selective blocker of GSK3β activity SB415286 for 24 h, and we measured gene expression. We also treated the F442A preadipocytes as a comparative white fat cell model. Since *Pparg2* is stably expressed after 24 h, we determined its expression in terminally differentiated adipocytes. As we previously showed [64], SB415286 inhibited *Pparg2* expression in F442A adipocytes (Fig. 6A). *Pparg2* expression was high in both EB5 and EB7 cells induced with RMD or SDR, as expected (Fig. 6B), and SB415286 inhibited it in EB5 and EB7 cells more when we induced the cells with SDR (about 90%) than with RMD (about 50%) (Fig. 6B). These results show that GSK3β activity is required for EB5 and EB7 as it is for F442A adipose differentiation, implying that this enzyme has a regulatory

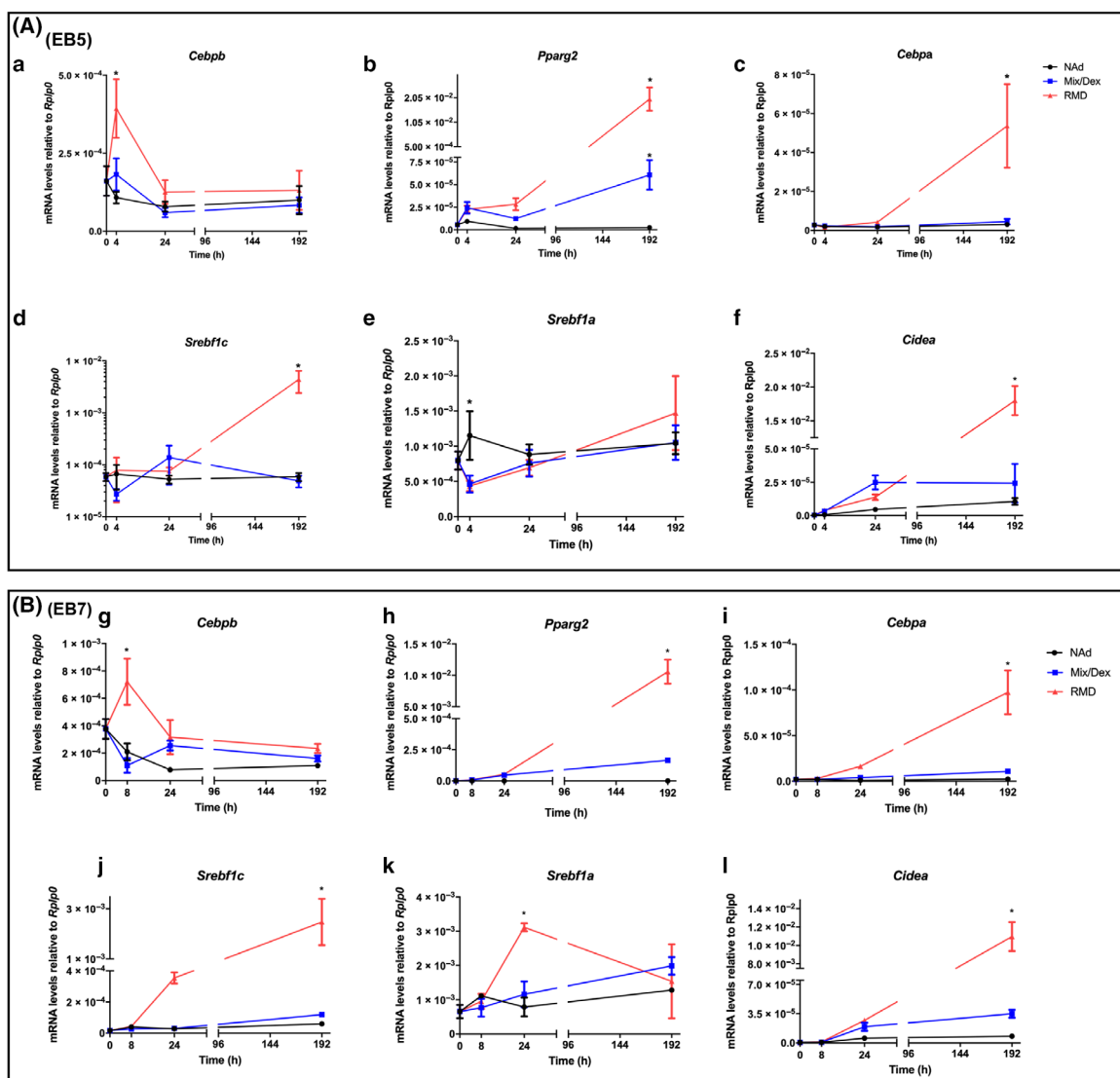


Fig. 5. Expression of adipogenic genes along the culture time in EB5 brown and EB7 brite cell clones. (A) EB5 cells. (B) EB7 cells. Confluent cultures were treated for 48 h with NAd, Mix/Dex, or RMD, and gene expression was measured using RT-PCR at various timepoints. The results are given as the mean \pm SEM of two triplicate experiments ($n = 6$). Asterisks indicate statistical differences with a P value ≤ 0.05 between the data groups, evaluated by ANOVA.

role in brown and brite adipogenesis, leading to the transcriptional adipogenic cascade expression.

Expression of lipid and carbohydrate metabolism genes in EB5 and EB7 adipocytes

Genes commonly expressed in the brown, brite, and white adipocytes: glucose and fatty acid uptake, lipogenesis, lipolysis, and intracytoplasmic fatty acid transport

Lpl, *Atgl*, *Lipe*, *Fasn*, *Gpdl*, and *Mlxipl* were all highly expressed in the adipocytes of the three clones when compared with the preadipocytes, as expected

(Fig. 7Aa,b). *Slc2a4* and *Fabp4* increased their expression in all three adipocytes compared to the preadipocytes, but *Cd36* only in EB5 and in EB7 but not in F442A adipocytes (Fig. 7Ac).

Genes selectively expressed in brown and brite adipocytes

Beta-oxidation

Relative to preadipocytes, *Cpt1b* expression increased about 1000-fold in the adipocytes of EB5 and EB7, but not in F442A adipocytes (Fig. 7Ba).

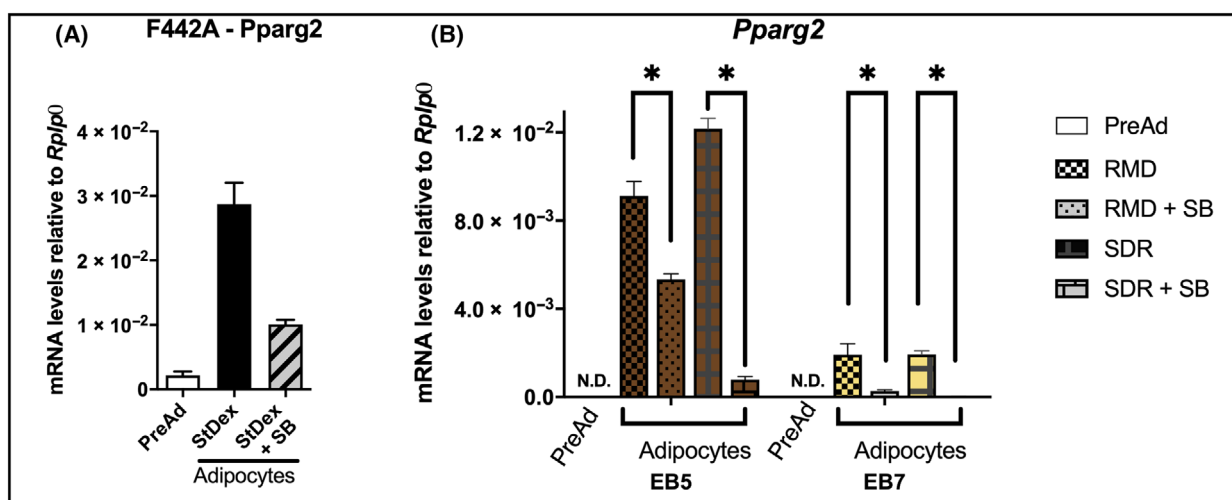


Fig. 6. SB415286 inhibits adipogenesis. (A) Postconfluent F442A cultures treated for 8 h with NAd, St/Dex, or St/Dex with SB415286 100 μ M. (B) Confluent cultures of EB5 or EB7 cells were treated for 48 h with NAd, SDR, or RMD with or without SB415286. *Pparg2* gene expression was measured using RT-PCR. The results are given as the mean \pm SEM of two triplicate experiments ($n = 6$). Asterisks denote a P value ≤ 0.05 between the two groups, evaluated by ANOVA.

Aacb increased its expression in the adipocytes in comparison with the preadipocytes in the three clones. While it only increased about 10-fold in F442A adipocytes, it increased by more than 1000-fold in EB5 and EB7 adipocytes (Fig. 7Bb), indicating it plays a crucial role in the brown and brite fat oxidation.

Mono-unsaturated fatty acid synthesis

Scd1 expression increased in EB5 and EB7 adipocytes, by about 1000-fold compared with preadipocytes, and only 10-fold in F442A adipocytes compared to preadipocytes (Fig. 7Bc), implying that brown and brite adipocytes would have a more active synthesis of MUFA than white adipocytes.

Adipokines

Adipoq (adiponectin) (Fig. 7Bd), and *Lep*, the gene encoding leptin (Fig. 7Be), increased their expression in EB5, EB7, and F442A adipocytes compared to their corresponding preadipocytes.

These results show that the EB5 and EB7 adipocytes have the metabolic pathways required for brown and brite fat cells to transport glucose and to provide fatty acids from different sources for mitochondrial beta-oxidation and energy expenditure, as seen in BAT and BRT. Additionally, we can expect that they are also engaged actively in the synthesis and signaling of both adipokines.

Discussion

Prior to our studies, it was not clear if brite progenitors arise during embryonic stages or after birth.

Brite adipocytes are activated after birth or during adulthood. As amply reviewed by Shao *et al.* [76], studies by different researchers in animal models have suggested, still controversially, that brite fat might arise via two possible mechanisms: (a) A white-to-brite fat and a brite-to-white transition, giving some support to the idea that brite adipocytes might remain dormant with a unilocular white adipocyte morphology. These results suggest that the differentiated adipocytes might have interchangeable morphologies under certain physiological or pharmacological conditions. (b) Specific precursors that undergo *de novo* differentiation into brite adipocytes after cold exposure, as supported by genetic tracing and lineage experiments.

Gupta and colleagues [76] recently proposed that brite adipocytes arise from cell progenitors through *de novo* brite adipogenesis during the first cold exposure. Subsequently, the cells interconvert between the dormant and the active brite phenotypes, a process called beige cell activation, in response to physiological or pharmacological stimulation. The interconversion between the dormant and the brite adipose phenotypes offer the benefit to rapidly respond to environmental changes [76]. Since we isolated the beige EB7 clone from 11–12 days mouse embryos, we demonstrated that cell progenitors for brite adipogenesis arise during early embryonic life. This is around the same time as the brown adipocytes and

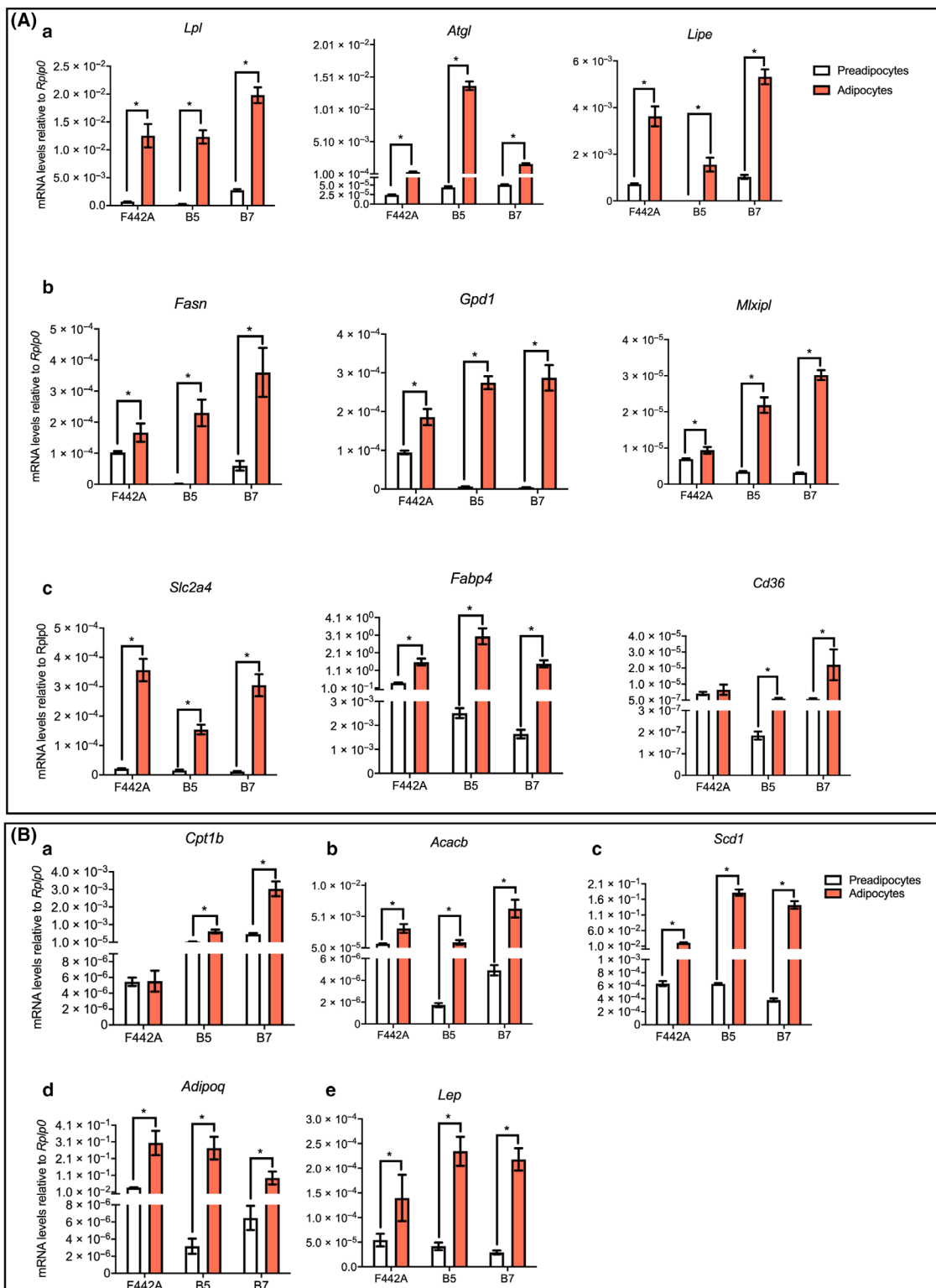


Fig. 7. (A) Expression of genes related to beta-oxidation and MUFA synthesis. Postconfluent cultures of F442A cells or confluent cultures of EB5 or EB7 cells were treated with NAd or RMD for 48 h, and gene expression was measured using RT-PCR after 192 h. (B) Expression of lipid and glucose metabolism genes and adipokines. Cultures treated as in panel A. The results are given as the mean \pm SEM of two triplicate experiments ($n = 6$). Asterisks indicate statistical differences with a P value ≤ 0.05 between the indicated data groups, evaluated by ANOVA.

earlier than white fat arises. We suggest that the brite adipose progenitors are well established during embryonic life, before the first cold exposure to activate brite fat. We cannot conclude if these progenitors undergo adipose differentiation in the embryo and then remain dormant as beige fat, or if they undergo adipogenesis after birth and the first cold stimulation.

As reported earlier, 4 h exposure to cold temperatures stimulated the expression of *Ucp1* and *Pparg1a* directly at the cellular level in white and beige adipocyte cell lines, but not in brown adipocyte cell lines [40]. In contrast, 10 °C cold exposure for 20 h induced *Ucp1* and *Pparg1a* expression in the intrascapular BAT in mice [40], whereas mice exposed to 4 °C for 2 h increased *Pparg1a* expression but not *Ucp1* expression in the interscapular BAT [61]. The discrepancy between these published *in vitro* and *in vivo* studies remains unresolved, but may be related to the different times and temperatures used in these studies. In our experiments, cold incubation of the EB7 adipocytes stimulated *Ucp1* and *Pparg1a* expression, consistent with a beige phenotype for EB7 cells. Cold exposure of EB5 adipocytes increased *Pparg1a* but not *Ucp1* expression, which is consistent with the *in vivo* studies of BAT [61]. However, this is in contrast to the immortalized brown clonal adipocytes isolated from the stromal vascular fraction, where cold-induced *Pparg1a* was not observed [40]. This discrepancy might be explained by clonal cell differences and/or the inherent heterogeneity of adipocyte populations, such as differences in genomic imprinting and/or temporal regulation of gene expression. This is not surprising, given that single-cell RNA sequencing in murine BAT cells showed distinct brown preadipocyte and adipocyte populations, indicating the presence of heterogenous adipocytes. For example, *Ucp1* expression greatly varies within individual adipocytes in morphologically uniform murine BAT [77]. Indeed, unstimulated EB5 cells expressed far more *Ucp1* than unstimulated EB7 cells and, as pointed out by Wang and Seale [78], under unstimulated conditions, brown adipocytes express relatively higher levels of UCP1 than beige adipocytes. Therefore, the data integration of the genetic markers expression and the *Ucp1*, *Pparg1a*, and *Fabp4* expression in response to cold support the conclusion that EB5 is of the brown fat lineage, and the EB7 is of the brite lineage.

Induction of adipogenesis

Cell differentiation is characterized by commitment, clonal expansion, and expression of the new phenotype (i.e., mature adipocytes). We attempted to study the molecular events leading to the induction of brown and

brite adipose commitment using small molecules that act intracellularly, circumventing the effect of serum adipogenic substances or other proteins on the cell surface. In the NAd medium, we promoted differentiation with either of two adipogenic cocktails: Mix/Dex/Ros and St/Dex/Ros. Because Ros in combination with Mix/Dex is widely used to stimulate browning in adipocytes, we also asked if Ros plays a role in commitment or in stimulating the brown and brite adipose phenotypes. Our results suggested that Mix/Dex or St/Dex induced commitment to differentiation. But the cells did not differentiate into adipocytes, as determined both genotypically and morphologically unless we added Ros to the medium. Ros alone, as a well-known agonist of PPAR γ , does not induce commitment, but it promotes the differentiation of the committed cells into the new adipose phenotype. It is poorly known if the action of Ros is exclusively related to PPAR γ activity or to other yet-unknown activities. In the 3T3-L1 and F442A, the white adipose clones, Ros enhances adipose differentiation, but it is not required to activate the full lipogenic program, since these cells seem to have an endogenous agonist of PPAR γ [79,80]. It is possible that the brown and brite fat clones have a low concentration, or do not have such intracellular agonists, and therefore Ros must be added to the culture medium to achieve full adipocyte differentiation. Indeed, Ros might have additional roles in brown and brite fat differentiation that are not yet known. We can conclude that Mix/Dex and St/Dex induce commitment to differentiate, whereas Ros promotes the differentiated brown and brite adipose phenotypes.

We showed that St/Dex rapidly induced, within 4 h exposure, the F442A cells to further differentiate to adipocytes [52,64]. We proposed that St induced two phases for differentiation before clonal expansion in the F442A cells. In the first stage of 4 h induction, St induced progenitor cells to initiate differentiation, and in the second phase of 44 h stabilization, the cells continued into differentiation without the inducer. After these two stages, the cells entered clonal expansion and expressed the adipose phenotype. Before the stabilization stage ends at the time of clonal amplification, it can still be manipulated with various substances to reverse commitment, restoring the cells to their preinduction state [52,64].

Induction with Mix/Dex and St/Dex of EB5 and EB7 for only 2 and 24 h, respectively, was enough for the cells to undergo full commitment. Our results with the EB5 and EB7 cells suggest that these similarities with the F442A cells hint that the brown and brite preadipocytes might go through similar intracellular molecular events of induction and stabilization before

clonal expansion. We can hypothesize that, after induction, stabilization will regulate the progression into differentiation and the generation of new adipocytes. An example is the addition of Ros after induction, i.e., the stabilization stage, stimulates the EB5 and EB7 clones to continue to full expression of the new adipose phenotype. It is not surprising that St is an inducer of cell commitment to differentiation. Besides our results that St induces commitment of F442A, EB5 and EB7, as we showed, and 3T3-L1 (unpublished results), it has been reported that stauprimide, an analog of St, induces differentiation of embryonic stem cells into the endoderm lineage [81]. All these results suggested that St, and some of its analogs, could induce differentiation in cell progenitors in various tissues or differentiation pathways.

Induction of adipogenesis depends on GSK3 β activity

St is a serine/threonine kinase inhibitor that activates GSK3 β [65], so inhibiting this kinase with lithium chloride or with the selective blocker SB415286 inhibited adipose differentiation of F442A cells [64]. Our experiments with the GSK3 β selective blocker SB415286 showed that *Pparg2* expression was inhibited in EB5 and EB7 cells more when induced with SDR (about 90%) than with RMD (about 50%). The results suggested that GSK3 β is also a crucial kinase in the brown and brite adipogenic pathways. However, since GSK3 β inhibition was lower when the cells were induced with RMD than with SDR, it would suggest that commitment with RMD might take place through additional signaling pathways that might not involve the activity of the kinase. Since both cell lines are clones, it is conceivable that the brown and brite adipogenic progenitors might undergo commitment through distinct regulatory steps, yet poorly known. These regulatory pathways would drive the cells to reach a common step, which could be the activation of the PRDM16-C/EBP β complex and the canonical transcriptional cascade gene expression [2,18,82].

Brown and brite adipogenesis might share some events with white adipogenesis to commit the progenitors into differentiation: (a) A signaling pathway mediated by GSK3 β activation that acts as a molecular switch for the differentiation of mesenchymal precursors into adipocytes. This pathway would link GSK3 β activity, phosphorylating, directly or indirectly, Thr¹⁷⁹ and Ser¹⁸⁴ of C/EBP β activating its DNA-binding function [64,83,84] to promote *Pparg2* and *Cebpa* transcription [85–87]. (b) Other signaling pathways, yet unknown, circumventing GSK3 β activity while leading

to C/EBP β activation and the expression of *Pparg2*, *Cebpa*, and *Srebf1c* as regulators of brown and brite lipogenic gene expression.

We can propose that the EB5 and EB7 clones are cell progenitors at a very early preadipocyte stage, but are not committed until GSK3 β or another signaling pathway is activated. Hence, it appears that Mix/Dex or St/Dex involves the induction of early genes and molecular events that occur after *Prdm16* expression but before *Cebpb*. In contrast, inhibiting GSK3 β activity in β -adrenergically stimulated brown mature adipocytes or cold-exposed mice increased the thermogenic genes *Fgf21*, *Ucp1*, *Dio2*, and *Ppargc1a* expression [75]. Therefore, GSK3 β , a multifunctional kinase involved in many cellular functions [88], seems to play two distinct roles in brown and brite fat differentiation. GSK3 β activity is crucial for the induction of adipogenesis in brown, brite, and white preadipocytes, but in contrast, it must be inhibited for β -adrenergic or cold stimulation of the thermogenic program in brown adipocytes, and not yet explored in brite adipocytes.

Srebf1a, the gene encoding another crucial transcription factor in white adipogenesis, SREBP1a [51], was expressed early in the brite cells, similarly to F442A preadipocytes, but less in the brown preadipocytes. *Srebf1a* knockdown during adipogenesis of the human SGBS preadipocyte cell strain, decreased the cell proliferation rate without inducing DNA damage or cell senescence, and without changing lipogenic gene expression. The PCR array of genes involved in cell cycle progression showed that SREBP1a could modulate 12 cell cycle-related genes [89]. It is conceivable that SREBP1a might have a role in the clonal amplification of the committed cells. Hence, it is tempting to speculate that SREBP1a might regulate the size of the fat lobules in the three adipose tissues, but limiting more the mass growth of the brown adipose organ. Another possible implication is that since *Srebf1a* is highly expressed in the early adipogenesis of the F442A and the EB7 cells, SREBP1a might influence WAT hyperplasia and mass size in obesity.

Lipid metabolism in EB5 and EB7 clones

Fatty acid availability for thermogenesis and beta-oxidation is essential for UCP1 proton transport activity in BAT and BRT. Indeed, for the EB5 and EB7 adipocytes to be active in thermogenesis and energy expenditure, the expression of genes involved in metabolic pathways providing fatty acids, such as the lipogenic, the lipolytic, and the glucose and fatty acid transport pathways, is crucial. Lipoprotein lipase serves as a key enzyme in white adipose tissue, catalyzing the hydrolysis

of triglycerides in the bloodstream into glycerol and fatty acids at the plasma membrane. This crucial reaction enables the fatty acids' entry into the cytoplasm, where they are used for intracellular triglyceride synthesis and storage. The essential function of LPL in the catabolism of circulating triglycerides is mirrored in the observed increase in *Lpl* expression across all three studied adipocyte types. This induction suggests that the brown EB5 and brite EB7 adipocytes have a pronounced ability to process bloodstream triglycerides, rendering fatty acids available for uptake and likely destined for mitochondrial import and subsequent energy dissipation.

Short-term cold exposure of mice promotes triglyceride plasma clearance by increasing the breakdown of LPL-mediated triglyceride-rich lipoproteins in the bloodstream and promoting fatty acid transport by CD36 into BAT [90]. While *Fabp4* expression increased during adipogenesis of all three cell lines, *Cd36* expression increased only in EB5 and EB7 adipocytes, but not in F442A adipocytes relative to preadipocytes. These data would suggest that *Cd36* might have the function of also promoting fatty acid transport in the EB5 and EB7 adipocytes linked to fatty acid uptake into mitochondria. Similarly, to the expression of *Cd36*, expression of *Cpt1b* showed a substantial increase in EB5 and EB7 adipocyte, whereas this upregulation was not observed in the F442A white adipocytes. CPT1b is the rate-limiting enzyme in the carnitine shuttle for transporting fatty acids into the mitochondria for beta-oxidation. It is a regulatory enzyme whose activity is closely linked to the enzyme CPT2, located at the inner mitochondrial membrane that translocates fatty acids from CPT1 into the mitochondrial matrix. BAT shows the highest CPT1 activity among other tissues examined in rats, liver, kidney, heart, white fat, and muscle [91], but its expression was unknown in BRT. Our results also showed that *Cpt1b* expression is indeed significant in brite fat. On the other hand, acetyl-CoA Carboxylases (ACCs) catalyze the formation of malonyl-CoA by carboxylation of Acetyl-CoA and malonyl-CoA is an important inhibitor of CPT1 activity. There are two isoforms in mammals: ACC1 and ACC2. Fasn is found in the cytosol and is involved in the synthesis of fatty acids, while ACC2 (gene *Acacb*) is found in the outer mitochondrial membrane and catalyzes the formation of malonyl-CoA (reviewed in Wang *et al.* [92]). The increase in *Acacb* expression in the adipocytes in comparison with their corresponding preadipocytes was about 500-fold for EB5, 1200-fold for EB7, while only 50-fold for F442A. It is possible that ACC2 activity could be crucial in brown and brite fat to regulate the thermogenic pathway by modulating the concentration

of malonyl-CoA, an inhibitor of CPT1b activity. For example, downregulation of *Acacb* would lead to a lower concentration of malonyl-CoA, preventing CPT1b inhibition to drive thermogenesis. Taken together, our results suggest that the coordination of the activities of CD36, CPT1b, and ACC2 is crucial to partition the fatty acids into mitochondria for thermogenesis in brown fat and remarkably in brite fat.

Stearoyl CoA desaturase-1 (*Scd1*) is a rate-limiting enzyme that catalyzes the biosynthesis of MUFA, palmitoleyl-CoA and oleyl-CoA from palmitoyl-CoA and stearoyl-CoA, respectively. Our analysis revealed a substantial upregulation of *Scd1* expression in EB5 and EB7 adipocytes compared to their respective preadipocytes, with the extent of this upregulation being notably more pronounced than in the F442A clone. These data suggest that *Scd1* must have a key function in BAT and BRT metabolism by providing these adipocytes with palmitoleic and oleic fatty acids. Dietary oleate partially compensated for hypothermia and hypoglycemia in the cold-exposed *Scd1*^{-/-} mice, suggesting an important role of MUFAs in thermoregulation [93]. It is compelling to suggest that finding ways to stimulate the activity of *Scd1* in BAT or BRT might promote thermogenesis and energy expenditure by providing MUFAs for beta-oxidation by UCP1. Indeed, the impaired temperature control in cold-exposed *Scd1*-deficient mice agrees with preserving or stimulating the activity of *Scd1* to drive thermogenesis. This is consistent with the observation that *Scd1* promotes adipose lipid mobilization in response to cold stimulation [94]. Experiments silencing the *Scd1* gene in the EB5 and EB7 adipocytes might show if *Scd1* deficiency might lead to a downregulation of *Ucp1* expression and thermogenesis in brown and brite adipocytes, and hence to assign a crucial role of *Scd1* to reroute the concentration of saturated fatty acids to MUFAs and the use of these for thermogenesis.

Since both EB5 and EB7 adipocytes express genes essential for various aspects of carbohydrate and lipid metabolism, it is important to determine their physiological competence. The β_3 -adrenergic response demonstrates the physiological capabilities of brown adipocytes, as indicated by lipolysis, UCP1 content, and oxygen consumption (refer to Introduction). We found that norepinephrine, a selective β_3 -AR agonist, increased UCP1 protein levels and lipolytic activity in EB5 brown and EB7 beige adipocytes, confirming their functional metabolic competence. Interestingly, the EB7 adipocytes, which are brite/beige adipocytes, also exhibited the selective β_3 -adrenergic response, suggesting that brite/beige adipose tissue likely responds to β_3 -adrenergic stimulation.

Conclusion

The EB5 and EB7 murine embryonic clonal cells differentiate into brown and brite adipocytes and express their corresponding tissue-specific gene markers. Interestingly, we also described the crucial role of GSK3 β , a molecular switch in various differentiation processes, to regulate brown and brite fat differentiation. Additionally, the differentiated adipocytes express the crucial genes of the carbohydrate, lipid, and thermogenic pathways of brown and brite fat. Studies using EB5 and EB7 should complement other models for exploring adipocyte biology. First, given that the cells are derived from 11 to 12 embryos, they may aid to better understand commitment, differentiation, and/or development of brown and beige cells. Second, these cell lines may be used to study crucial enzymes involved in lipid and carbohydrate metabolism and discern how different adipocyte populations make different contributions to metabolism. Third, these cells may be useful to identify and/or characterize drug candidates targeting energy expenditure for treating obesity and related metabolic complications. In sum, the ability to perform large-scale cultivation with clonally pure EB5 and EB7 cells should aid in studies-related developmental biology, intermediary metabolism, and/or drug discovery.

Acknowledgements

The authors thank Dr James Lenhard for his helpful comments and suggestions while drafting the article. Resources came from WKH laboratory at CINVESTAV. Castro-Rodriguez, L.I., and Vazquez-Sandoval, A., were recipients of a CONACyT PhD fellowships. During the preparation of this work the author(s) used Chat GPT 4.0 to improve readability and language use. The author(s) reviewed and edited the Chat GPT 4.0-generated output and take full responsibility for the content of the publication.

Conflict of interest

The authors declare they own stock in a start-up biotech company. CV-V is a consultant. WK-H is a founder and serves on the board without pay. These relationships have been disclosed and have not influenced the content of this article.

Data accessibility

The authors confirm that the data supporting the findings of this study are available within the article and its supplementary materials.

Author contributions

WK-H and CV-V designed the experiments. CV-V, MM-M, CPH-M, LIC-R, and AV-S performed the experiments. CV-V and WK-H analyzed the data. CV-V and WK-H wrote the article. All authors read and approved the final article.

References

- Scheele C and Wolfrum C (2021) Functional diversity of human adipose tissue revealed by spatial mapping. *Nat Rev Endocrinol* **17**, 713–714.
- Seale P, Bjork B, Yang W, Kajimura S, Chin S, Kuang S, Scime A, Devarakonda S, Conroe HM, Erdjument-Bromage H *et al.* (2008) PRDM16 controls a brown fat/skeletal muscle switch. *Nature* **454**, 961–967.
- Cousin B, Cinti S, Morrioni M, Raimbault S, Ricquier D, Penicaud L and Casteilla L (1992) Occurrence of brown adipocytes in rat white adipose tissue: molecular and morphological characterization. *J Cell Sci* **103** (Pt 4), 931–942.
- Jespersen NZ, Larsen TJ, Pejjs L, Daugaard S, Homoe P, Loft A, de Jong J, Mathur N, Cannon B, Nedergaard J *et al.* (2013) A classical brown adipose tissue mRNA signature partly overlaps with brite in the supraclavicular region of adult humans. *Cell Metab* **17**, 798–805.
- Lidell ME, Betz MJ, Dahlqvist Leinhard O, Heglind M, Elander L, Slawik M, Mussack T, Nilsson D, Romu T, Nuutila P *et al.* (2013) Evidence for two types of brown adipose tissue in humans. *Nat Med* **19**, 631–634.
- Sharp LZ, Shinoda K, Ohno H, Scheel DW, Tomoda E, Ruiz L, Hu H, Wang L, Pavlova Z, Gilsanz V *et al.* (2012) Human BAT possesses molecular signatures that resemble beige/brite cells. *PLoS One* **7**, e49452.
- Cypess AM, White AP, Vernochet C, Schulz TJ, Xue R, Sass CA, Huang TL, Roberts-Toler C, Weiner LS, Sze C *et al.* (2013) Anatomical localization, gene expression profiling and functional characterization of adult human neck brown fat. *Nat Med* **19**, 635–639.
- Wu J, Bostrom P, Sparks LM, Ye L, Choi JH, Giang AH, Khandekar M, Virtanen KA, Nuutila P, Schaart G *et al.* (2012) Beige adipocytes are a distinct type of thermogenic fat cell in mouse and human. *Cell* **150**, 366–376.
- Calderon-Dominguez M, Sebastian D, Fucho R, Weber M, Mir JF, Garcia-Casarrubios E, Obregon MJ, Zorzano A, Valverde AM, Serra D *et al.* (2016) Carnitine palmitoyltransferase 1 increases lipolysis, UCP1 protein expression and mitochondrial activity in brown adipocytes. *PLoS One* **11**, e0159399.
- Himms-Hagen J, Cui J, Danforth E Jr, Taatjes DJ, Lang SS, Waters BL and Claus TH (1994) Effect of CL-316,243, a thermogenic beta 3-agonist, on energy balance and brown and white adipose tissues in rats. *Am J Physiol* **266**, R1371–R1382.

- 11 Seale P, Conroe HM, Estall J, Kajimura S, Frontini A, Ishibashi J, Cohen P, Cinti S and Spiegelman BM (2011) Prdm16 determines the thermogenic program of subcutaneous white adipose tissue in mice. *J Clin Invest* **121**, 96–105.
- 12 Cypess AM and Kahn CR (2010) The role and importance of brown adipose tissue in energy homeostasis. *Curr Opin Pediatr* **22**, 478–484.
- 13 Tseng YH, Cypess AM and Kahn CR (2010) Cellular bioenergetics as a target for obesity therapy. *Nat Rev Drug Discov* **9**, 465–482.
- 14 Kajimura S, Spiegelman BM and Seale P (2015) Brown and beige fat: physiological roles beyond heat generation. *Cell Metab* **22**, 546–559.
- 15 Bargut TCL, Souza-Mello V, Aguila MB and Mandarim-de-Lacerda CA (2017) Browning of white adipose tissue: lessons from experimental models. *Horm Mol Biol Clin Investig* **31**, doi: [10.1515/hmbci-2016-0051](https://doi.org/10.1515/hmbci-2016-0051)
- 16 Cypess AM, Lehman S, Williams G, Tal I, Rodman D, Goldfine AB, Kuo FC, Palmer EL, Tseng YH, Doria A *et al.* (2009) Identification and importance of brown adipose tissue in adult humans. *N Engl J Med* **360**, 1509–1517.
- 17 Lepper C and Fan CM (2010) Inducible lineage tracing of Pax7-descendant cells reveals embryonic origin of adult satellite cells. *Genesis* **48**, 424–436.
- 18 Kajimura S, Seale P, Kubota K, Lunsford E, Frangioni JV, Gygi SP and Spiegelman BM (2009) Initiation of myoblast to brown fat switch by a PRDM16-C/EBP-beta transcriptional complex. *Nature* **460**, 1154–1158.
- 19 Wang QA, Tao C, Gupta RK and Scherer PE (2013) Tracking adipogenesis during white adipose tissue development, expansion and regeneration. *Nat Med* **19**, 1338–1344.
- 20 Schulz TJ, Huang TL, Tran TT, Zhang H, Townsend KL, Shadrach JL, Cerletti M, McDougall LE, Giorgadze N, Tchekonia T *et al.* (2011) Identification of inducible brown adipocyte progenitors residing in skeletal muscle and white fat. *Proc Natl Acad Sci USA* **108**, 143–148.
- 21 Lee YH and Granneman JG (2012) Seeking the source of adipocytes in adult white adipose tissues. *Adipocyte* **1**, 230–236.
- 22 Oguri Y, Shinoda K, Kim H, Alba DL, Bolus WR, Wang Q, Brown Z, Pradhan RN, Tajima K, Yoneshiro T *et al.* (2020) CD81 controls beige fat progenitor cell growth and energy balance via FAK signaling. *Cell* **182**, 563–577.e20.
- 23 Wolfrum C and Straub LG (2018) Lessons from Cre-mice and indicator mice. *Handb Exp Pharmacol* **251**, 37–54.
- 24 Kong X, Williams KW and Liu T (2017) Genetic mouse models: the powerful tools to study fat tissues. *Methods Mol Biol* **1566**, 99–107.
- 25 Hepler C, Vishvanath L and Gupta RK (2017) Sorting out adipocyte precursors and their role in physiology and disease. *Genes Dev* **31**, 127–140.
- 26 Reznikoff CA, Brankow DW and Heidelberger C (1973) Establishment and characterization of a cloned line of C3H mouse embryo cells sensitive to postconfluence inhibition of division. *Cancer Res* **33**, 3231–3238.
- 27 Lenhard JM, Kliewer SA, Paulik MA, Plunket KD, Lehmann JM and Weiel JE (1997) Effects of troglitazone and metformin on glucose and lipid metabolism: alterations of two distinct molecular pathways. *Biochem Pharmacol* **54**, 801–808.
- 28 Rodriguez-Cano MM, Gonzalez-Gomez MJ, Sanchez-Solana B, Monsalve EM, Diaz-Guerra MM, Laborda J, Nueda ML and Baladron V (2020) NOTCH receptors and DLK proteins enhance brown adipogenesis in mesenchymal C3H10T1/2 cells. *Cells* **9**, 2032.
- 29 Cao Y, Liu X, Zhao J and Du M (2021) AMPKalpha regulates Idh2 transcription through H2B O-GlcNAcylation during brown adipogenesis. *Acta Biochim Biophys Sin (Shanghai)* **53**, 112–118.
- 30 Xue R, Wan Y, Zhang S, Zhang Q, Ye H and Li Y (2014) Role of bone morphogenetic protein 4 in the differentiation of brown fat-like adipocytes. *Am J Physiol Endocrinol Metab* **306**, E363–E372.
- 31 Imran KM, Yoon D and Kim YS (2017) A pivotal role of AMPK signaling in medicarpin-mediated formation of brown and beige adipocytes from C3H10T1/2 mesenchymal stem cells. *Biofactors* **44**, 168–179.
- 32 Imran KM, Yoon D, Lee TJ and Kim YS (2018) Medicarpin induces lipolysis via activation of protein kinase a in brown adipocytes. *BMB Rep* **51**, 249–254.
- 33 Wang H, Willershauser M, Karlas A, Gorpas D, Reber J, Ntziachristos V, Maurer S, Fromme T, Li Y and Klingenspor M (2019) A dual Ucp1 reporter mouse model for imaging and quantitation of brown and brite fat recruitment. *Mol Metab* **20**, 14–27.
- 34 Rahman MS, Imran KM, Hossain M, Lee TJ and Kim YS (2021) Biochanin A induces a brown-fat phenotype via improvement of mitochondrial biogenesis and activation of AMPK signaling in murine C3H10T1/2 mesenchymal stem cells. *Phytother Res* **35**, 920–931.
- 35 Iuchi S, Marsch-Moreno M, Velez-DelValle C, Easley K, Kuri-Harcuch W and Green H (2006) An immortalized drug-resistant cell line established from 12-13-day mouse embryos for the propagation of human embryonic stem cells. *Differentiation* **74**, 160–166.
- 36 Green H and Kehinde O (1974) Sublines of mouse 3T3 cells that accumulate lipid. *Cell* **1**, 113–116.
- 37 Green H and Kehinde O (1975) An established preadipose cell line and its differentiation in culture. II. Factors affecting the adipose conversion. *Cell* **5**, 19–27.

- 38 de Jong JM, Larsson O, Cannon B and Nedergaard J (2015) A stringent validation of mouse adipose tissue identity markers. *Am J Physiol Endocrinol Metab* **308**, E1085–E1105.
- 39 Petrovic N, Walden TB, Shabalina IG, Timmons JA, Cannon B and Nedergaard J (2010) Chronic peroxisome proliferator-activated receptor gamma (PPARgamma) activation of epididymally derived white adipocyte cultures reveals a population of thermogenically competent, UCP1-containing adipocytes molecularly distinct from classic brown adipocytes. *J Biol Chem* **285**, 7153–7164.
- 40 Ye L, Wu J, Cohen P, Kazak L, Khandekar MJ, Jedrychowski MP, Zeng X, Gygi SP and Spiegelman BM (2013) Fat cells directly sense temperature to activate thermogenesis. *Proc Natl Acad Sci USA* **110**, 12480–12485.
- 41 Zhao J, Unelius L, Bengtsson T, Cannon B and Nedergaard J (1994) Coexisting beta-adrenoceptor subtypes: significance for thermogenic process in brown fat cells. *Am J Physiol* **267**, C969–C979.
- 42 Rohlf s EM, Daniel KW, Premont RT, Kozak LP and Collins S (1995) Regulation of the uncoupling protein gene (Ucp) by beta 1, beta 2, and beta 3-adrenergic receptor subtypes in immortalized brown adipose cell lines. *J Biol Chem* **270**, 10723–10732.
- 43 Chaudhry A and Granneman JG (1999) Differential regulation of functional responses by beta-adrenergic receptor subtypes in brown adipocytes. *Am J Physiol* **277**, R147–R153.
- 44 Fain JN, Jacobs MD and Clement-Cormier YC (1973) Interrelationship of cyclic AMP, lipolysis, and respiration in brown fat cells. *Am J Physiol* **224**, 346–351.
- 45 Chan SS and Fain JN (1970) Uncoupling action of sulfonyleureas on brown fat cells. *Mol Pharmacol* **6**, 513–523.
- 46 Nedergaard J and Lindberg O (1979) Norepinephrine-stimulated fatty-acid release and oxygen consumption in isolated hamster brown-fat cells. Influence of buffers, albumin, insulin and mitochondrial inhibitors. *Eur J Biochem* **95**, 139–145.
- 47 Matthias A, Ohlson KB, Fredriksson JM, Jacobsson A, Nedergaard J and Cannon B (2000) Thermogenic responses in brown fat cells are fully UCP1-dependent. UCP2 or UCP3 do not substitute for UCP1 in adrenergically or fatty acid-induced thermogenesis. *J Biol Chem* **275**, 25073–25081.
- 48 Cero C, Lea HJ, Zhu KY, Shamsi F, Tseng YH and Cypess AM (2021) beta3-adrenergic receptors regulate human brown/beige adipocyte lipolysis and thermogenesis. *JCI Insight* **6**, e139160.
- 49 Li Y, Fromme T, Schweizer S, Schottl T and Klingenspor M (2014) Taking control over intracellular fatty acid levels is essential for the analysis of thermogenic function in cultured primary brown and brite/beige adipocytes. *EMBO Rep* **15**, 1069–1076.
- 50 Todaro GJ and Green H (1963) Quantitative studies of the growth of mouse embryo cells in culture and their development into established lines. *J Cell Biol* **17**, 299–313.
- 51 Ayala-Sumuano JT, Velez-Del Valle C, Beltran-Langarica A, Hernandez JM and Kuri-Harcuch W (2008) Adipogenic genes on induction and stabilization of commitment to adipose conversion. *Biochem Biophys Res Commun* **374**, 720–724.
- 52 Diaz-Velasquez CE, Castro-Munozledo F and Kuri-Harcuch W (2008) Staurosporine rapidly commits 3T3-F442A cells to the formation of adipocytes by activation of GSK-3beta and mobilization of calcium. *J Cell Biochem* **105**, 147–157.
- 53 Kuri-Harcuch W and Green H (1978) Adipose conversion of 3T3 cells depends on a serum factor. *Proc Natl Acad Sci USA* **75**, 6107–6109.
- 54 Ramirez-Zacarias JL, Castro-Munozledo F and Kuri-Harcuch W (1992) Quantitation of adipose conversion and triglycerides by staining intracytoplasmic lipids with Oil red O. *Histochemistry* **97**, 493–497.
- 55 Pruitt KD, Brown GR, Hiatt SM, Thibaud-Nissen F, Astashyn A, Ermolaeva O, Farrell CM, Hart J, Landrum MJ, McGarvey KM *et al.* (2014) RefSeq: an update on mammalian reference sequences. *Nucleic Acids Res* **42**, D756–D763.
- 56 Johnson M, Zaretskaya I, Raytselis Y, Merezuk Y, McGinnis S and Madden TL (2008) NCBI BLAST: a better web interface. *Nucleic Acids Res* **36**, W5–W9.
- 57 Hernandez-Mosqueira C, Velez-delValle C and Kuri-Harcuch W (2015) Tissue alkaline phosphatase is involved in lipid metabolism and gene expression and secretion of adipokines in adipocytes. *Biochim Biophys Acta* **1850**, 2485–2496.
- 58 Kiefer FW, Vernochet C, O'Brien P, Spoerl S, Brown JD, Nallamshetty S, Zeyda M, Stulnig TM, Cohen DE, Kahn CR *et al.* (2012) Retinaldehyde dehydrogenase 1 regulates a thermogenic program in white adipose tissue. *Nat Med* **18**, 918–925.
- 59 Merlin J, Sato M, Nowell C, Pakzad M, Fahey R, Gao J, Dehvari N, Summers RJ, Bengtsson T, Evans BA *et al.* (2018) The PPARgamma agonist rosiglitazone promotes the induction of brite adipocytes, increasing beta-adrenoceptor-mediated mitochondrial function and glucose uptake. *Cell Signal* **42**, 54–66.
- 60 Morrison RF and Farmer SR (1999) Insights into the transcriptional control of adipocyte differentiation. *J Cell Biochem Suppl* **32–33**, 59–67.
- 61 Lockie SH, Heppner KM, Chaudhary N, Chabenne JR, Morgan DA, Veyrat-Durebex C, Ananthakrishnan G, Rohner-Jeanrenaud F, Drucker DJ, DiMarchi R *et al.* (2012) Direct control of brown adipose tissue

- thermogenesis by central nervous system glucagon-like peptide-1 receptor signaling. *Diabetes* **61**, 2753–2762.
- 62 Russell TR and Ho R (1976) Conversion of 3T3 fibroblasts into adipose cells: triggering of differentiation by prostaglandin F₂alpha and 1-methyl-3-isobutyl xanthine. *Proc Natl Acad Sci USA* **73**, 4516–4520.
- 63 Gregoire FM, Smas CM and Sul HS (1998) Understanding adipocyte differentiation. *Physiol Rev* **78**, 783–809.
- 64 Ayala-Sumuano JT, Velez-Delvalle C, Beltran-Langarica A, Marsch-Moreno M, Cerbon-Solorzano J and Kuri-Harcuch W (2011) Srebf1a is a key regulator of transcriptional control for adipogenesis. *Sci Rep* **1**, 178.
- 65 Koivisto L, Alavian K, Hakkinen L, Pelech S, McCulloch CA and Larjava H (2003) Glycogen synthase kinase-3 regulates formation of long lamellipodia in human keratinocytes. *J Cell Sci* **116**, 3749–3760.
- 66 Ohno H, Shinoda K, Spiegelman BM and Kajimura S (2012) PPARgamma agonists induce a white-to-brown fat conversion through stabilization of PRDM16 protein. *Cell Metab* **15**, 395–404.
- 67 Aune UL, Ruiz L and Kajimura S (2013) Isolation and differentiation of stromal vascular cells to beige/brite cells. *J Vis Exp* **73**, 50191.
- 68 Cao Z, Umek RM and McKnight SL (1991) Regulated expression of three C/EBP isoforms during adipose conversion of 3T3-L1 cells. *Genes Dev* **5**, 1538–1552.
- 69 Tontonoz P, Hu E, Graves RA, Budavari AI and Spiegelman BM (1994) mPPAR gamma 2: tissue-specific regulator of an adipocyte enhancer. *Genes Dev* **8**, 1224–1234.
- 70 Birsoy K, Chen Z and Friedman J (2008) Transcriptional regulation of adipogenesis by KLF4. *Cell Metab* **7**, 339–347.
- 71 Oishi Y, Manabe I, Tobe K, Tsushima K, Shindo T, Fujii K, Nishimura G, Maemura K, Yamauchi T, Kubota N *et al.* (2005) Kruppel-like transcription factor KLF5 is a key regulator of adipocyte differentiation. *Cell Metab* **1**, 27–39.
- 72 Cervantes-Camacho C, Beltran-Langarica A, Ochoa-Uribe AK, Marsch-Moreno M, Ayala-Sumuano JT, Velez-delValle C and Kuri-Harcuch W (2015) The transient expression of Klf4 and Klf5 during adipogenesis depends on GSK3beta activity. *Adipocyte* **4**, 248–255.
- 73 Jash S, Banerjee S, Lee MJ, Farmer SR and Puri V (2019) CIDEA transcriptionally regulates UCPI for browning and thermogenesis in human fat cells. *iScience* **20**, 73–89.
- 74 Liu X and Yao Z (2016) Chronic over-nutrition and dysregulation of GSK3 in diseases. *Nutr Metab (Lond)* **13**, 49.
- 75 Markkussen LK, Winther S, Wicksteed B and Hansen JB (2018) GSK3 is a negative regulator of the thermogenic program in brown adipocytes. *Sci Rep* **8**, 3469.
- 76 Shao M, Wang QA, Song A, Vishvanath L, Busbuso NC, Scherer PE and Gupta RK (2019) Cellular origins of beige fat cells revisited. *Diabetes* **68**, 1874–1885.
- 77 Karlina R, Lutter D, Miok V, Fischer D, Altun I, Schottl T, Schorpp K, Israel A, Cero C, Johnson JW *et al.* (2021) Identification and characterization of distinct brown adipocyte subtypes in C57BL/6J mice. *Life Sci Alliance* **4**, e202000924.
- 78 Wang W and Seale P (2016) Control of brown and beige fat development. *Nat Rev Mol Cell Biol* **17**, 691–702.
- 79 Tzamelis I, Fang H, Ollero M, Shi H, Hamm JK, Kievit P, Hollenberg AN and Flier JS (2004) Regulated production of a peroxisome proliferator-activated receptor-gamma ligand during an early phase of adipocyte differentiation in 3T3-L1 adipocytes. *J Biol Chem* **279**, 36093–36102.
- 80 Hallenborg P, Petersen RK, Kouskoumvekaki I, Newman JW, Madsen L and Kristiansen K (2016) The elusive endogenous adipogenic PPARgamma agonists: lining up the suspects. *Prog Lipid Res* **61**, 149–162.
- 81 Zhu S, Wurdak H, Wang J, Lyssiotis CA, Peters EC, Cho CY, Wu X and Schultz PG (2009) A small molecule primes embryonic stem cells for differentiation. *Cell Stem Cell* **4**, 416–426.
- 82 Kajimura S, Seale P and Spiegelman BM (2010) Transcriptional control of brown fat development. *Cell Metab* **11**, 257–262.
- 83 Tang QQ, Otto TC and Lane MD (2003) CCAAT/enhancer-binding protein beta is required for mitotic clonal expansion during adipogenesis. *Proc Natl Acad Sci USA* **100**, 850–855.
- 84 Tang QQ, Gronborg M, Huang H, Kim JW, Otto TC, Pandey A and Lane MD (2005) Sequential phosphorylation of CCAAT enhancer-binding protein beta by MAPK and glycogen synthase kinase 3beta is required for adipogenesis. *Proc Natl Acad Sci USA* **102**, 9766–9771.
- 85 Christy RJ, Kaestner KH, Geiman DE and Lane MD (1991) CCAAT/enhancer binding protein gene promoter: binding of nuclear factors during differentiation of 3T3-L1 preadipocytes. *Proc Natl Acad Sci USA* **88**, 2593–2597.
- 86 Tang QQ and Lane MD (1999) Activation and centromeric localization of CCAAT/enhancer-binding proteins during the mitotic clonal expansion of adipocyte differentiation. *Genes Dev* **13**, 2231–2241.
- 87 Zhu Y, Qi C, Korenberg JR, Chen XN, Noya D, Rao MS and Reddy JK (1995) Structural organization of mouse peroxisome proliferator-activated receptor

- gamma (mPPAR gamma) gene: alternative promoter use and different splicing yield two mPPAR gamma isoforms. *Proc Natl Acad Sci USA* **92**, 7921–7925.
- 88 Beurel E, Grieco SF and Jope RS (2015) Glycogen synthase kinase-3 (GSK3): regulation, actions, and diseases. *Pharmacol Ther* **148**, 114–131.
- 89 Alvarez MS, Fernandez-Alvarez A, Cucarella C and Casado M (2014) Stable SREBP-1a knockdown decreases the cell proliferation rate in human preadipocyte cells without inducing senescence. *Biochem Biophys Res Commun* **447**, 51–56.
- 90 Bartelt A, Bruns OT, Reimer R, Hohenberg H, Ittrich H, Peldschus K, Kaul MG, Tromsdorf UI, Weller H, Waurisch C *et al.* (2011) Brown adipose tissue activity controls triglyceride clearance. *Nat Med* **17**, 200–205.
- 91 Doh K-O, Kim Y-W, Park S-Y, Lee S-K, Park JS and Kim J-Y (2005) Interrelation between long-chain fatty acid oxidation rate and carnitine palmitoyltransferase 1 activity with different isoforms in rat tissues. *Life Sci* **77**, 435–443.
- 92 Wang Y, Yu W, Li S, Guo D, He J and Wang Y (2022) Acetyl-CoA carboxylases and diseases. *Front Oncol* **12**, 836058.
- 93 Lee SH, Dobrzyn A, Dobrzyn P, Rahman SM, Miyazaki M and Ntambi JM (2004) Lack of stearoyl-CoA desaturase 1 upregulates basal thermogenesis but causes hypothermia in a cold environment. *J Lipid Res* **45**, 1674–1682.
- 94 Zou Y, Wang YN, Ma H, He ZH, Tang Y, Guo L, Liu Y, Ding M, Qian SW and Tang QQ (2020) SCD1 promotes lipid mobilization in subcutaneous white adipose tissue. *J Lipid Res* **61**, 1589–1604.
- 95 Ayala-Sumuano JT, Velez-delValle C, Beltran-Langarica A, Marsch-Moreno M, Hernandez-Mosqueira C and Kuri-Harcuch W (2013) Glucocorticoid paradoxically recruits adipose progenitors and impairs lipid homeostasis and glucose transport in mature adipocytes. *Sci Rep* **3**, 2573.
- 96 Wang YX, Lee CH, Tjep S, Yu RT, Ham J, Kang H and Evans RM (2003) Peroxisome-proliferator-activated receptor delta activates fat metabolism to prevent obesity. *Cell* **113**, 159–170.
- 97 Shimomura I, Shimano H, Horton JD, Goldstein JL and Brown MS (1997) Differential expression of exons 1a and 1c in mRNAs for sterol regulatory element binding protein-1 in human and mouse organs and cultured cells. *J Clin Invest* **99**, 838–845.

Supporting information

Additional supporting information may be found online in the Supporting Information section at the end of the article.

Table S1. Names, and acronyms of proteins and genes accordingly to the NCBI GenBank and GenPept databases.